Results and Implications of Benchmark Studies

Frank Simon
MPI for Physics & Excellence Cluster 'Universe'
Munich, Germany

CLIC CDR Review, Manchester, UK, October 2011

Max-Planck-Institut für Physik
(Werner-Heisenberg-Institut)

Excellence Cluster
Universe

Overview

- Intro: Goals of the Benchmark Studies
- Performance for Benchmark Processes
  - 3 TeV Benchmarks
    - Light Higgs
    - Heavy Higgs
    - Right Squarks
    - Charginos & Neutralinos
    - Sleptons
  - 500 GeV Benchmark
    - Top Pair Production
- Summary

Benchmark Studies - Goals

- Demonstrate the detector performance for physics observables
  - Use complete detector system
  - Realistic machine and SM background levels

- Processes to test various aspects of detector requirements at CLIC
  - Reconstruction of highly energetic jets and missing energy
  - Events with high jet multiplicity
  - Flavor tagging in a high background environment
  - Momentum reconstruction for high-energy leptons

- Studied at 3 TeV: The most challenging conditions
- One process at 500 GeV for direct comparison to ILC performance studies

Benchmarks - The Chosen Scenarios I

- Two SUSY scenarios with non-unified gaugino masses - Chosen to illustrate detector performance, emphasis on high-mass states for the 3 TeV case

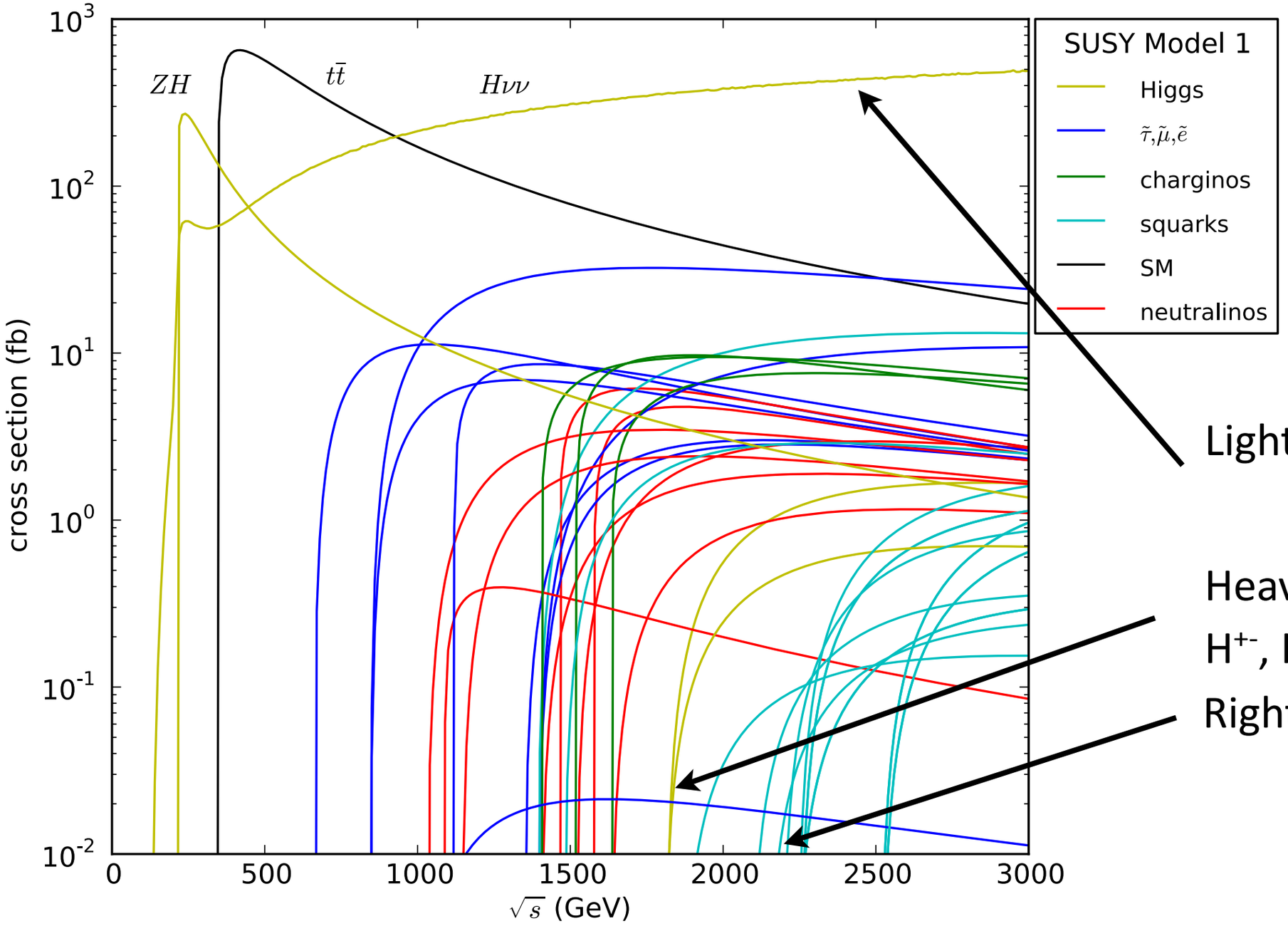

Model 1:
Squarks within CLIC 3 TeV reach, heavy neutral and charged Higgs

Light Higgs in W Fusion

Heavy Higgs:
H^{+-}, H^0A^0

Right Squarks

Benchmarks - The Chosen Scenarios II

- Two SUSY scenarios with non-unified gaugino masses - Chosen to illustrate detector performance, emphasis on high-mass states for the 3 TeV case

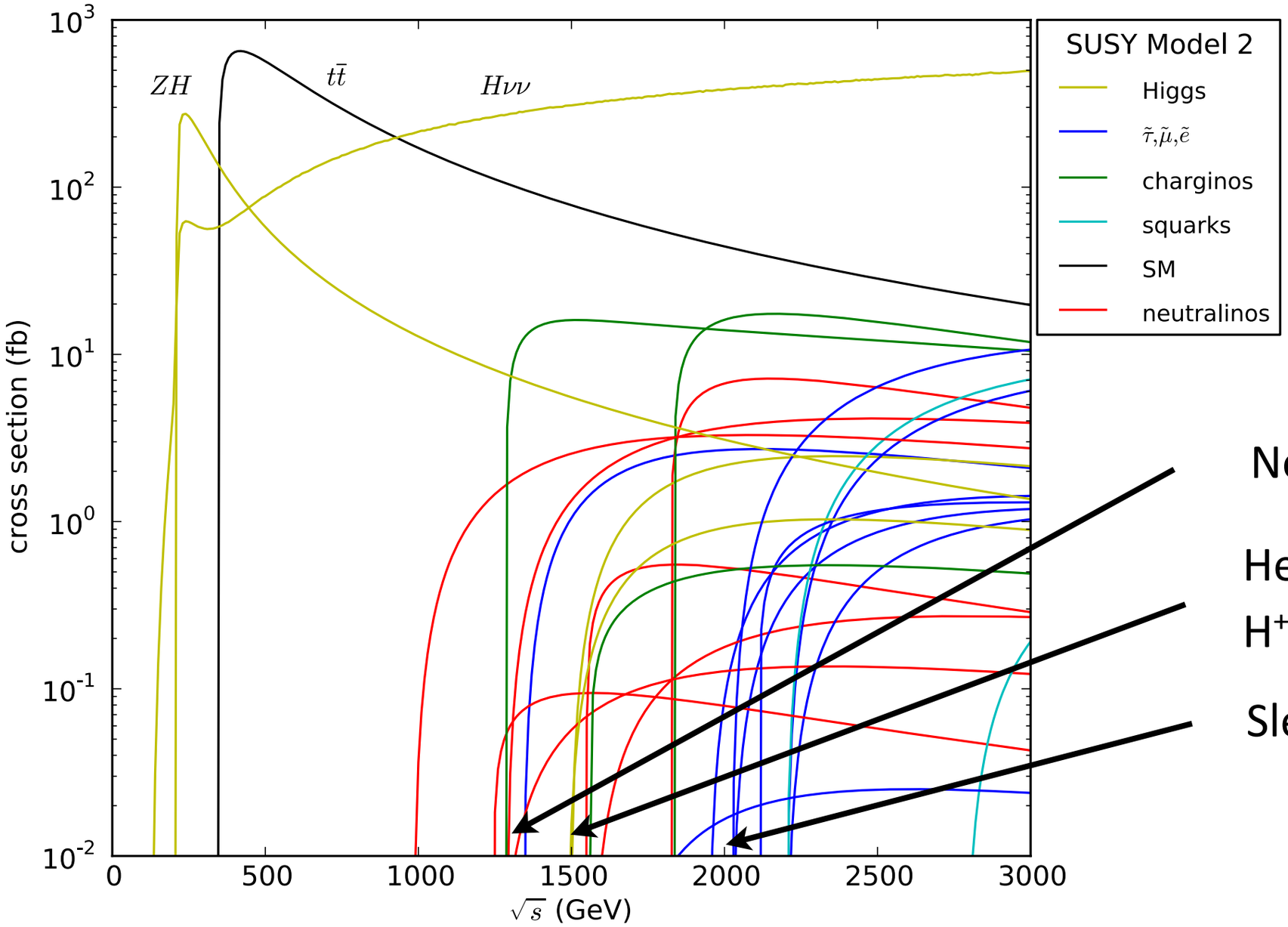

Model 2:
High mass sleptons,
Light charginos and neutralinos dominated by single decay mode

Neutralinos, Charginos

Heavy Higgs:
H^{+-}, H^0A^0

Sleptons

3 TeV Benchmarks

All studies:

- Assumed integrated luminosity of 2 ab^{-1}
- Full detector simulations

Light Higgs Production

- Higgs production in WW fusion has a high cross section at 3 TeV:
  420 fb (larger than maximum cross section for ZH slightly above threshold)
  Possibility for precise studies of Higgs decays -
  Mass dependence of coupling to fermions

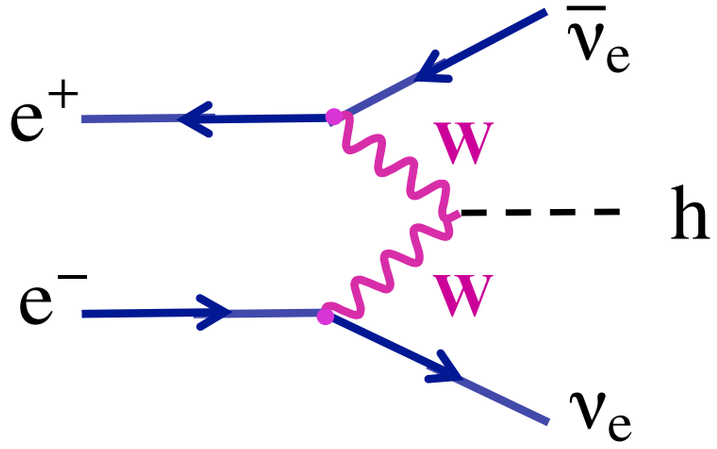

branching ratio into bb, cc (68%, 3.6%) $\mu^+\mu^-$ (0.03%)

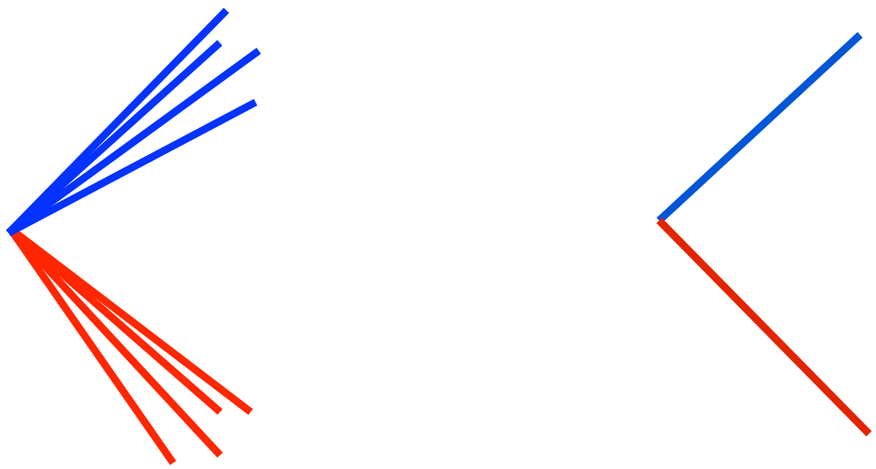

light Higgs mass: 120 GeV

Key detector performance aspects:
- Muon momentum reconstruction
- Flavor tagging for low-energy jets
- Jet energy reconstruction for low-energy jets

CLIC_SiD

Light Higgs - Hadronic Decays

- The main analysis challenge: Suppression of SM background, mainly W, Z, cross sections *O*(10 pb)
  - Higgs decay to bb: 285 fb, to cc: 15 fb

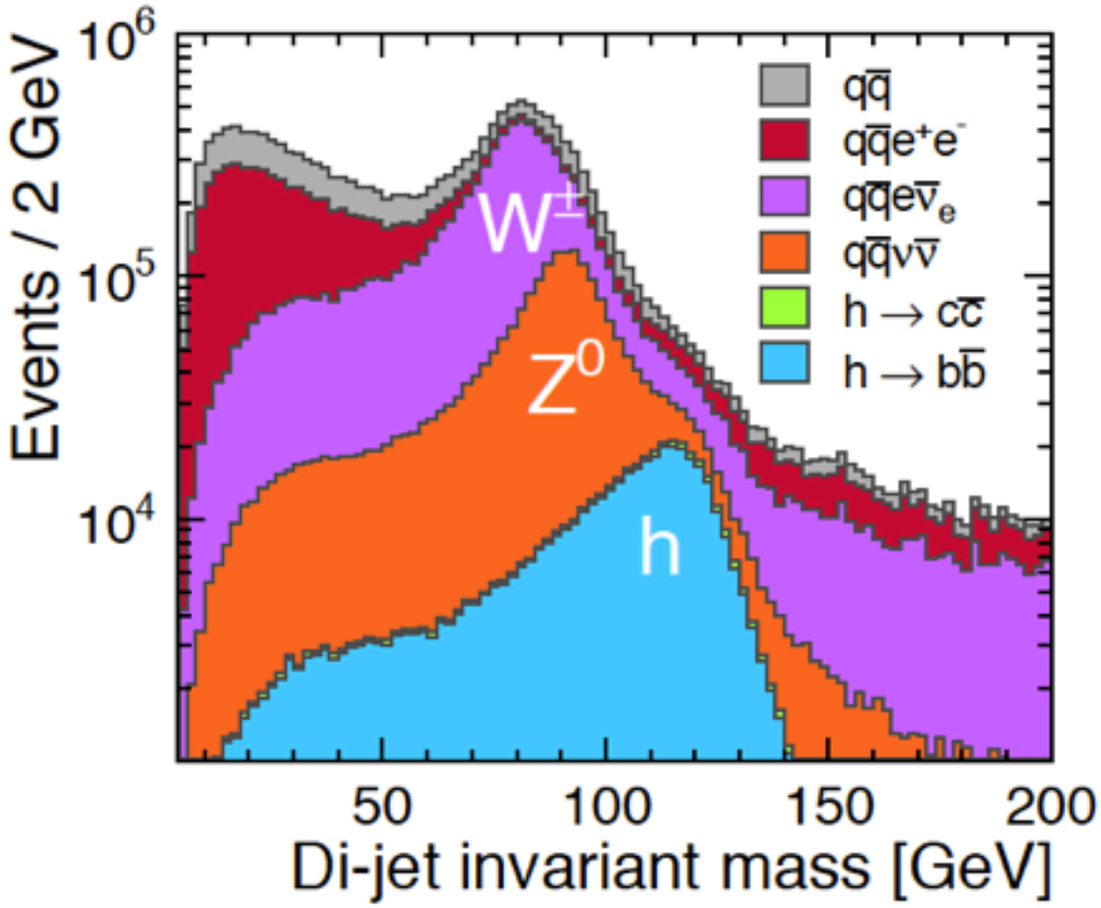

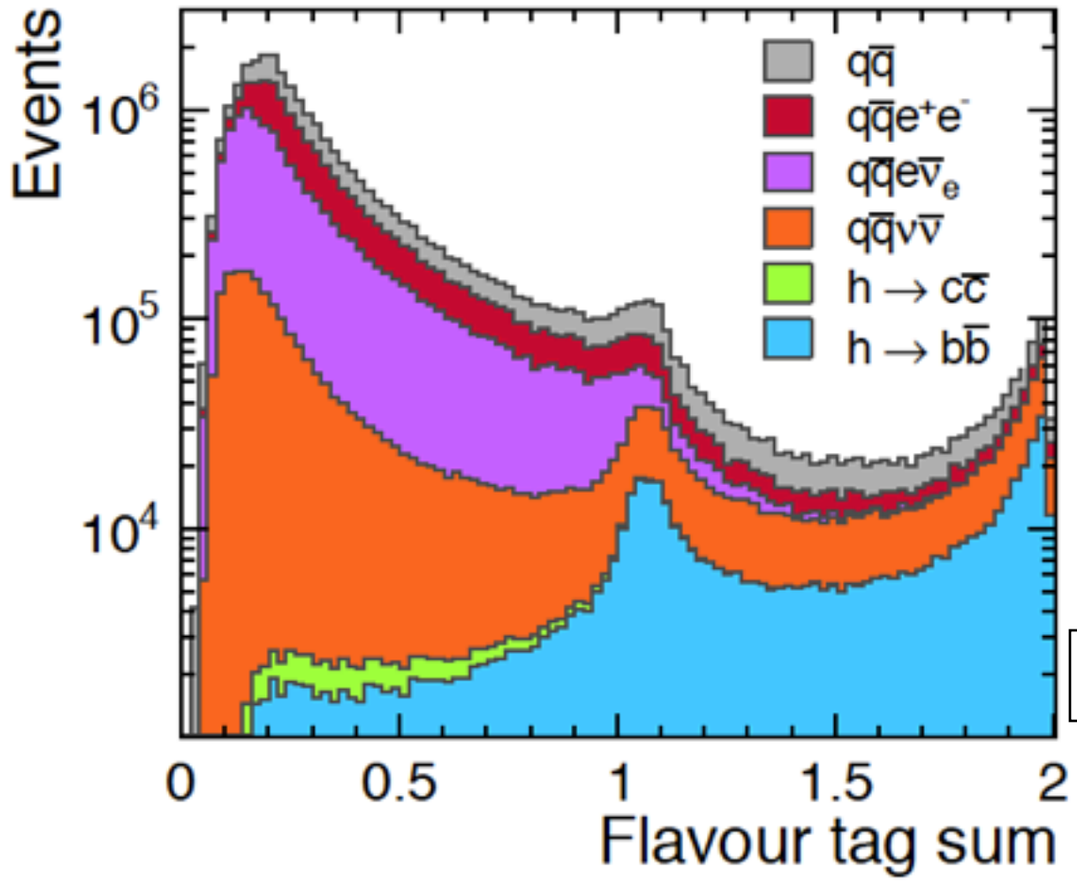

Fig. 12.14

(b - tagging)

- Background rejection based on Neural Network
  - most discriminating variables: Di-jet invariant mass, flavor tagging

Light Higgs - Hadronic Decays

- NN selection - Optimized for lowest statistical error

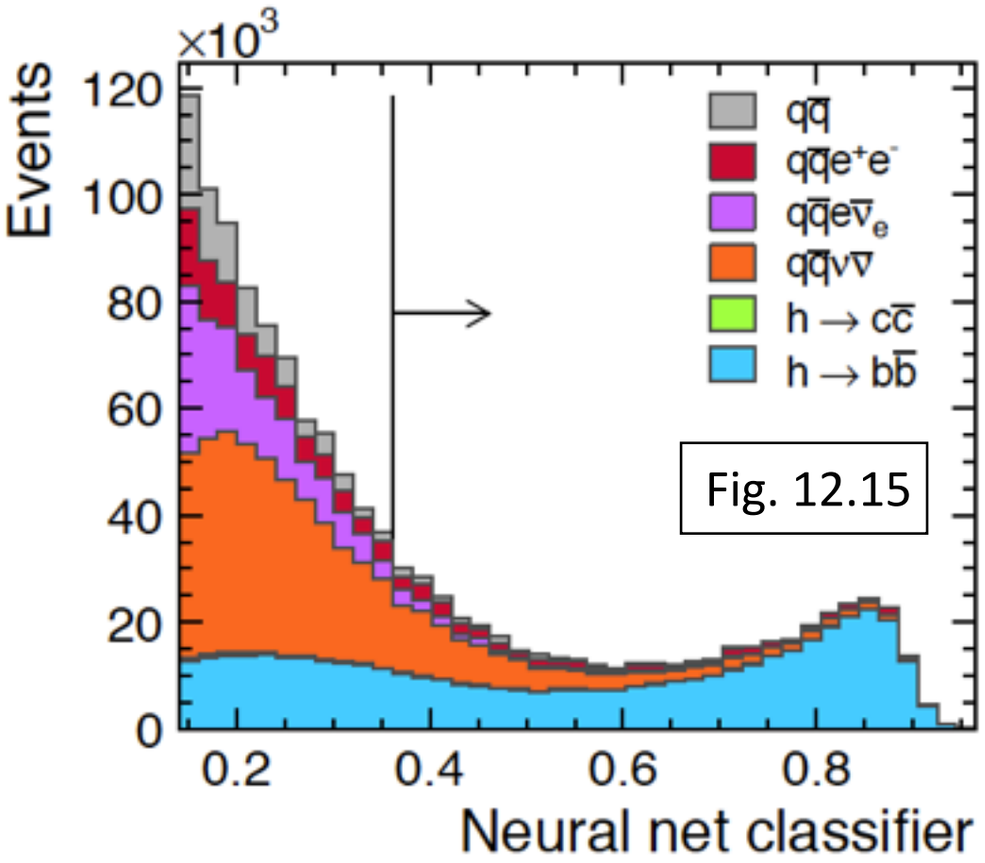

Fig. 12.15

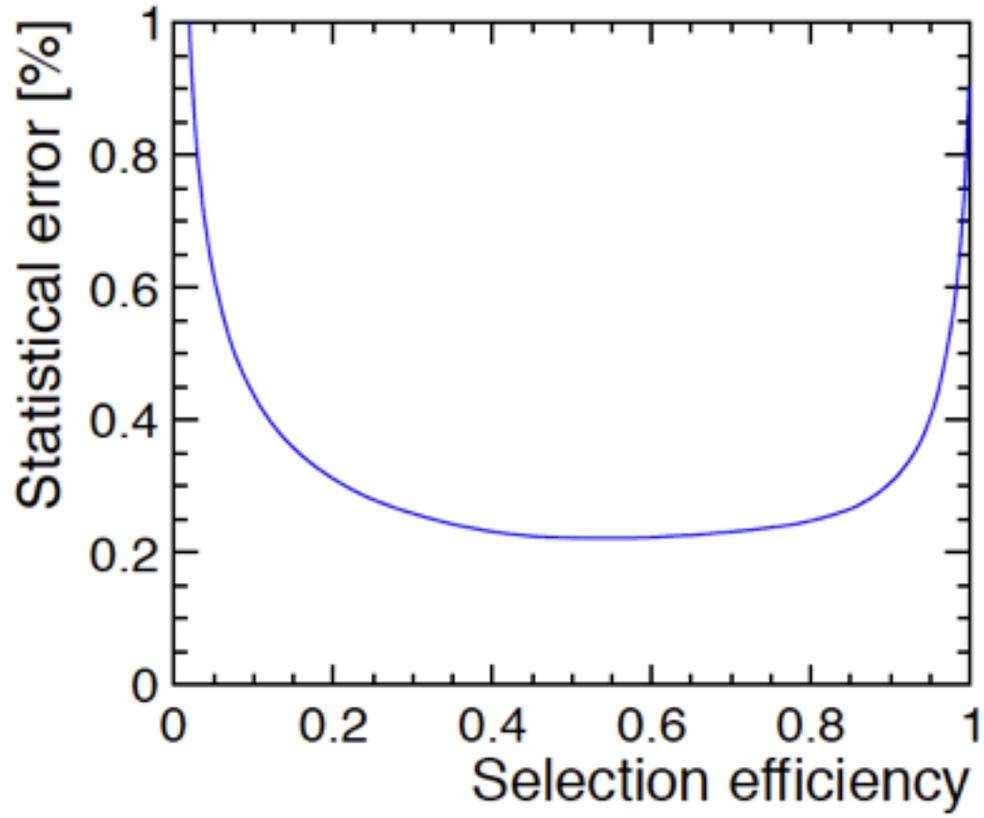

Fig. 12.16

- Analysis for cc final state using c-tag instead of b-tag
  - More challenging flavor tagging - reduced efficiency

	$h \to b\bar{b}$	$h \to c\bar{c}$
Signal purity	65.4%	24.1%
Signal efficiency	54.6%	15.2%
cross section statistical uncertainty	0.22%	3.24%

Light Higgs - Decay into Muons

- The main analysis challenge: Suppression of non-Higgs background, main contributions: $\mu^+\mu^-\nu\nu$ (irreducible, 132 fb), $\mu^+\mu^-e^+e^-$ (5.4 pb) (signal: 0.12 fb)

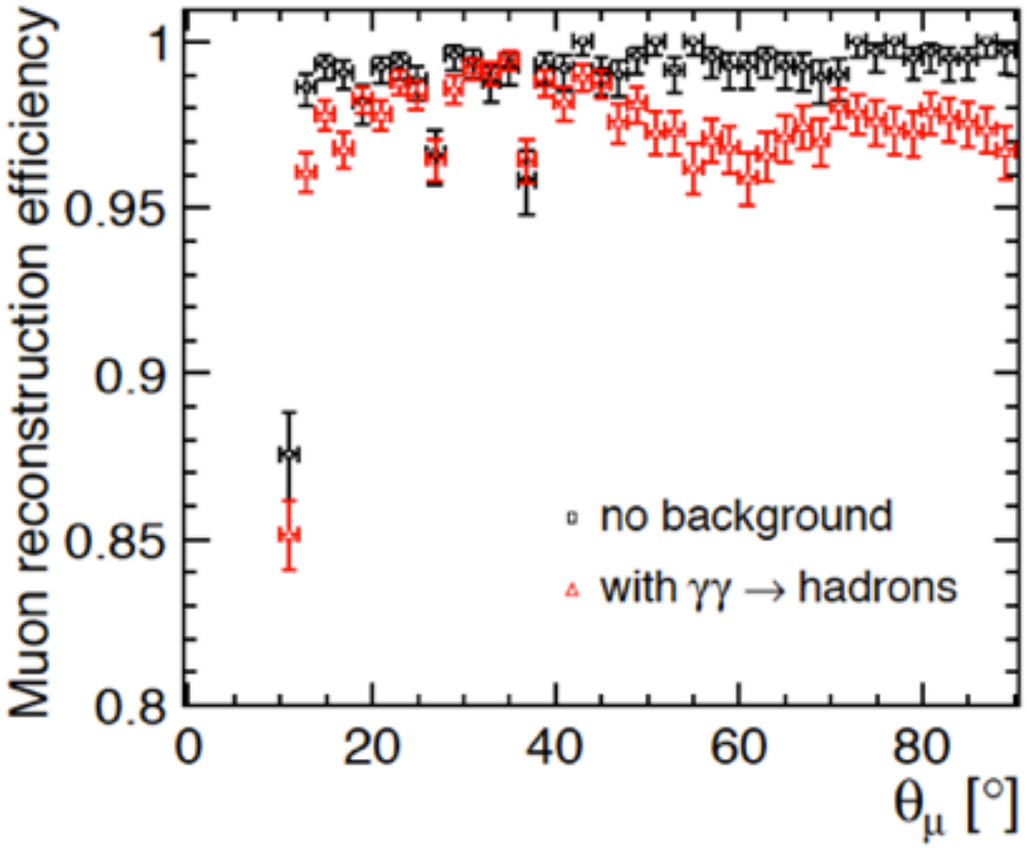

Acceptance given by tracker acceptance: 88% (no tracking below 10°)

Fig. 12.17

Light Higgs - Decay into Muons

- The main analysis challenge: Suppression of non-Higgs background, main contributions: $\mu^+\mu^-\nu\nu$ (irreducible, 132 fb), $\mu^+\mu^-e^+e^-$ (5.4 pb) (signal: 0.12 fb)

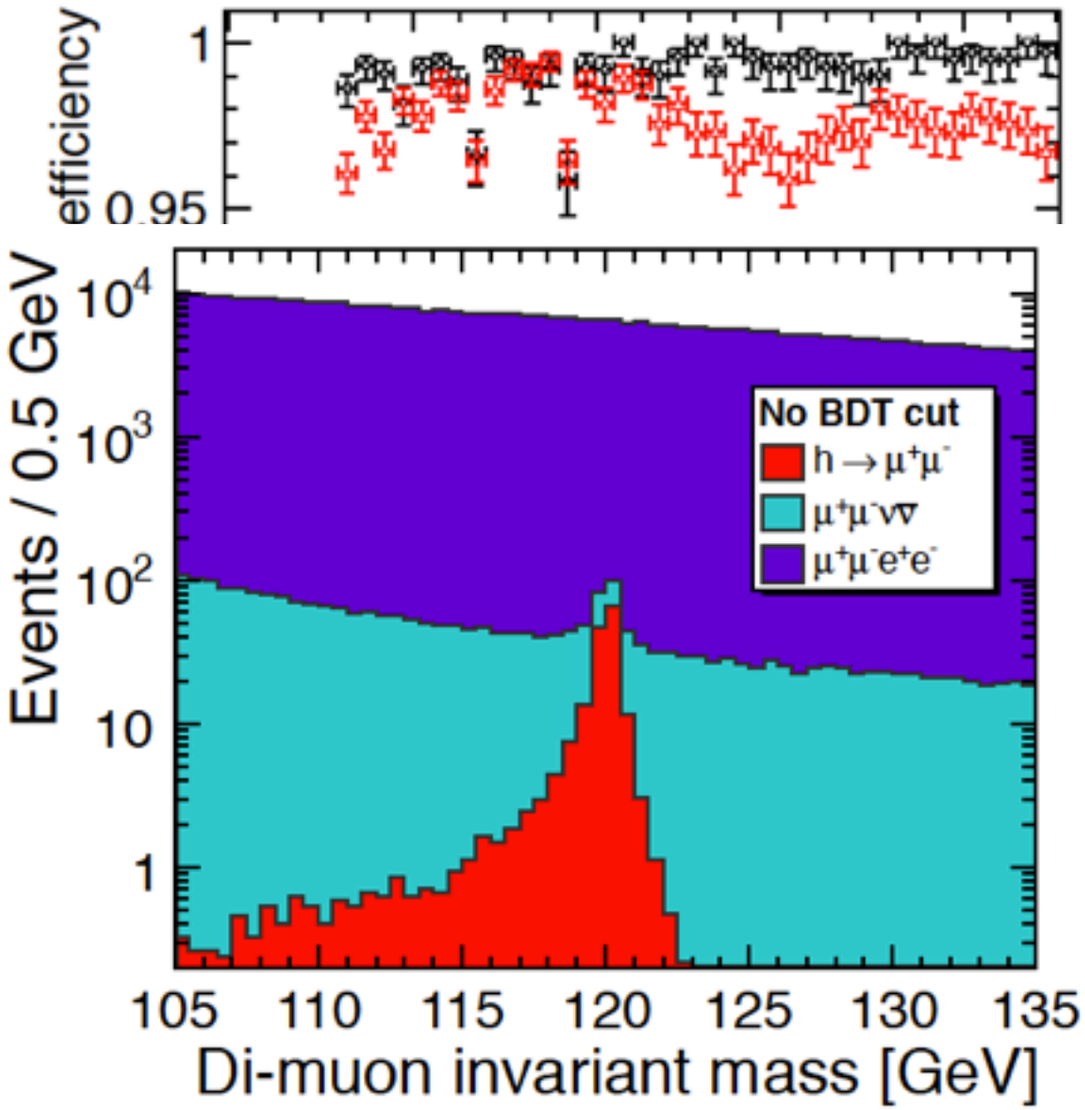

Acceptance given by tracker acceptance: 88% (no tracking below 10°)

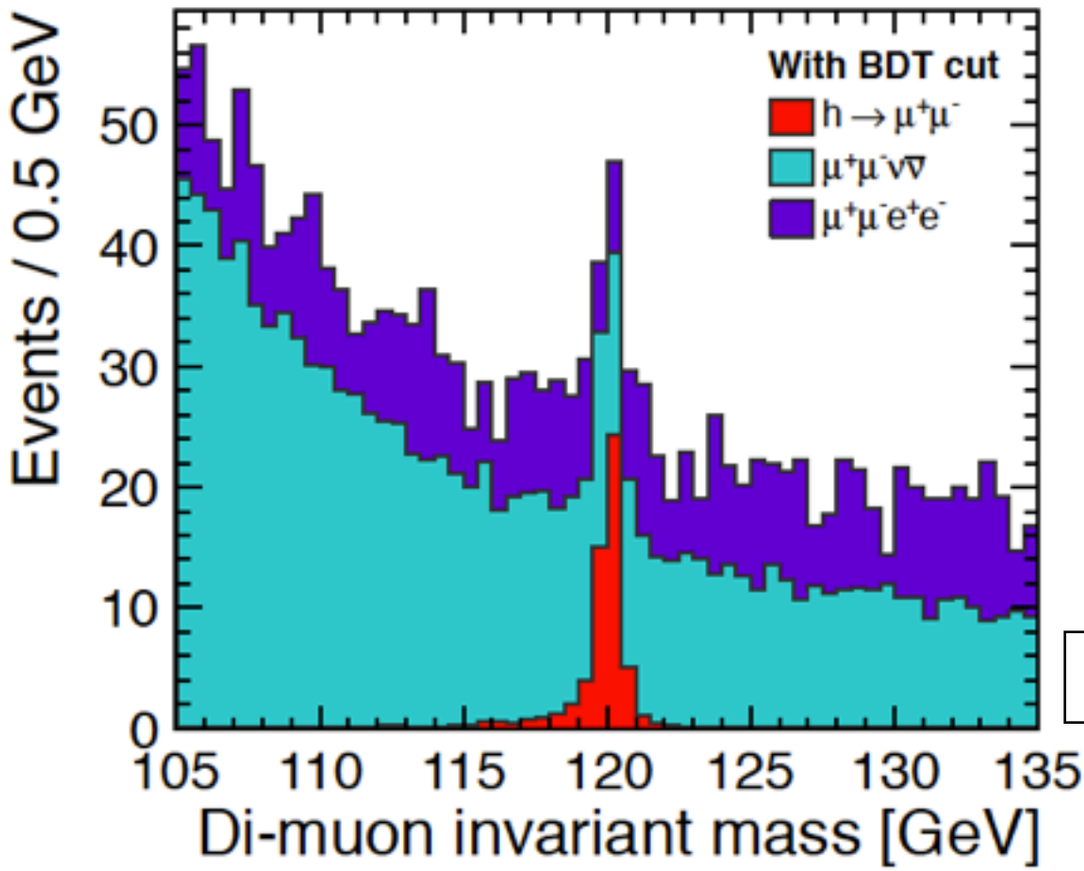

Fig. 12.18

High background level, in particular from $\mu^+\mu^-e^+e^-$, can be controlled with a Boosted Decision Tree

Light Higgs - Decay into Muons

- Clear signal, modeled by two half Gaussians
- Flat $\mu^+\mu^-e^+e^-$ background, exponential $\mu^+\mu^-\nu\nu$ background

Measurement accuracy determined via toy MC (100 trials) based on the signal and background pdfs

	$h \to \mu^+\mu^-$
Signal events	62 ± 14
Signal efficiency	25%
$\sigma_{h\nu_e\bar{\nu}_e} \times BR_{h\to\mu^+\mu^-}$	0.122 fb
Stat. uncertainty	23%

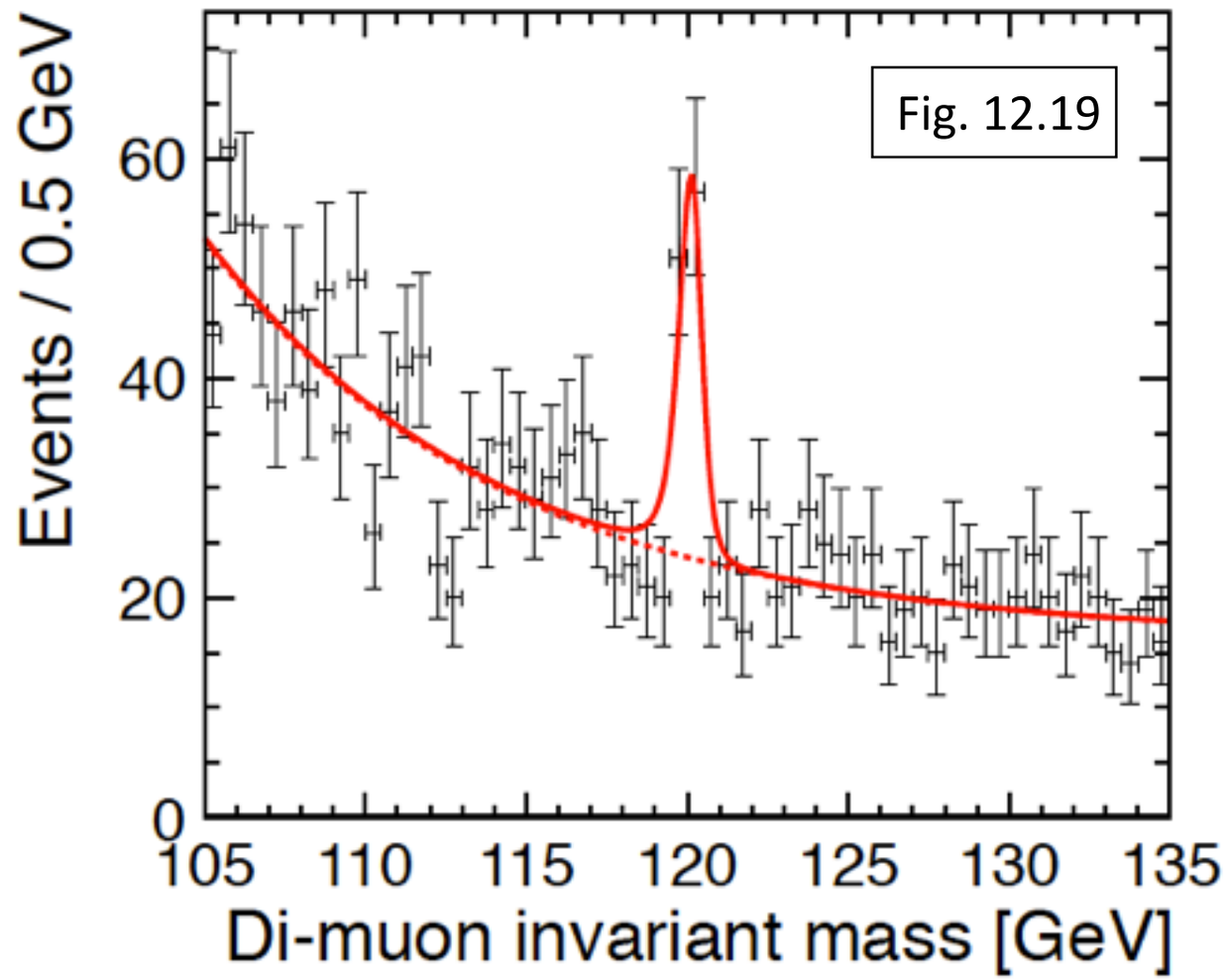

Light Higgs - Decay into Muons

- Clear signal, modeled by two half Gaussians
- Flat $\mu^+\mu^-e^+e^-$ background, exponential $\mu^+\mu^-\nu\nu$ background

Measurement accuracy determined via toy MC (100 trials) based on the signal and background pdfs

	$h \to \mu^+\mu^-$
Signal events	62 ± 14
Signal efficiency	25%
$\sigma_{h\nu_e\bar{\nu}_e} \times BR_{h\to\mu^+\mu^-}$	0.122 fb
Stat. uncertainty	23%

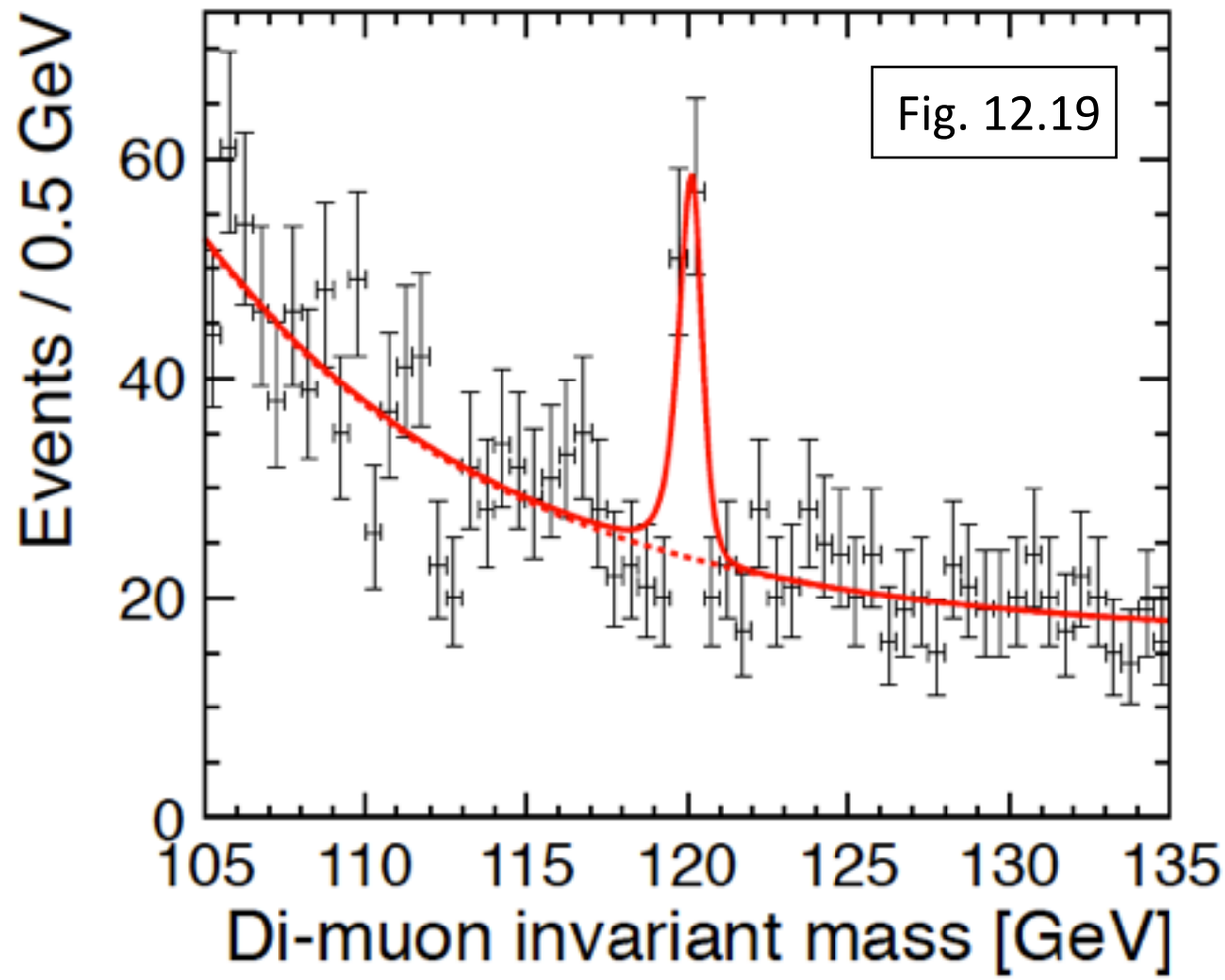

Further improvement expected from future inclusion of forward calorimeters to improve rejection of $\mu^+\mu^-e^+e^-$ background

Heavy Higgs Production

- Studies in SUSY model I & II:

  Heavy SUSY Higgs sector - Mass and width measurements

  - Predominant decay of neutral Higgs into b quarks

    $$e^+e^- \rightarrow H^0A^0 \rightarrow b\bar{b}b\bar{b}$$

  - Predominant decay of charged Higgs into t b

    $$e^+e^- \rightarrow H^+H^- \rightarrow t\bar{b}b\bar{t}$$

  - Neutral and charged Higgs are nearly mass degenerate around 905 GeV in Model I, 745 GeV in Model II

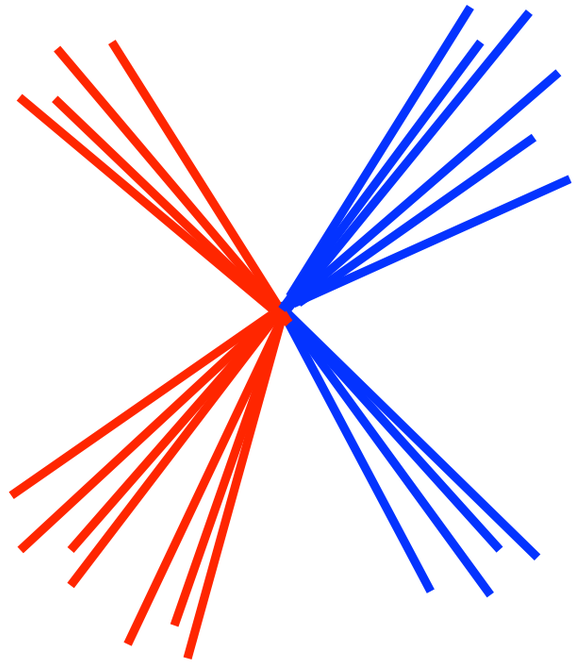

Key detector performance aspects:

- Flavor tagging for high-energy jets
- Invariant mass reconstruction of high mass states in a high multiplicity environment
- Identification of boosted top quarks from jet substructure

CLIC_ILD

Heavy Higgs Analysis

- Overall analysis strategy:
  - Cuts on visible energy and event shapes to reject SUSY events with missing energy and two fermion final states
  - Flavor tagging - 4 b jets in the final state
  - Top tagging using jet substructure and jet mass
  - Kinematic fit using transverse momentum and beam energy constraints (allowing for beamstrahlung)
  - Equal mass of di-jet systems to resolve jet pairing ambiguities and to further improve mass resolution

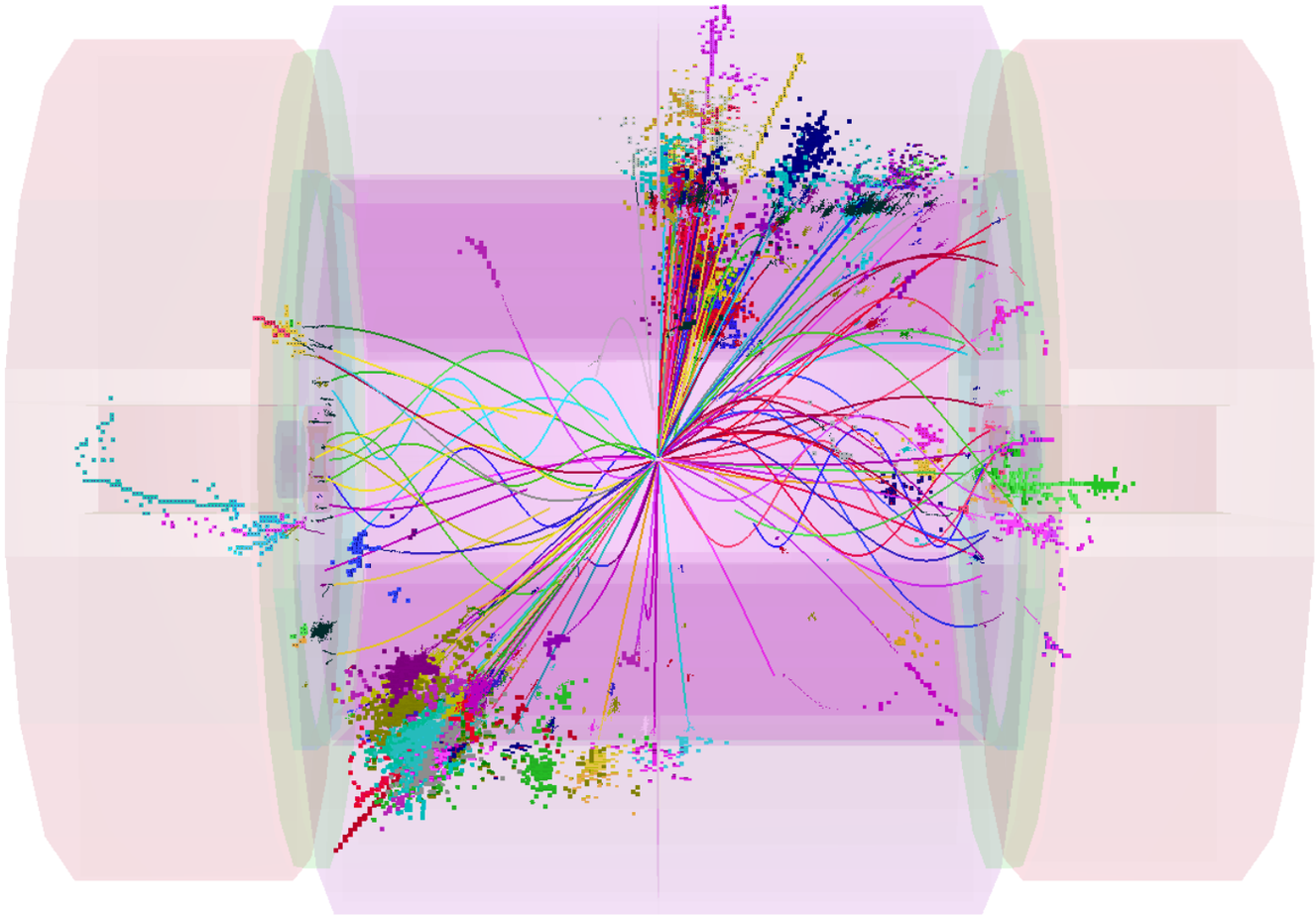

$e^+e^- \rightarrow H^+H^- \rightarrow t\bar{b}\bar{b}\bar{t}$

8-Jet event

Heavy Higgs Results

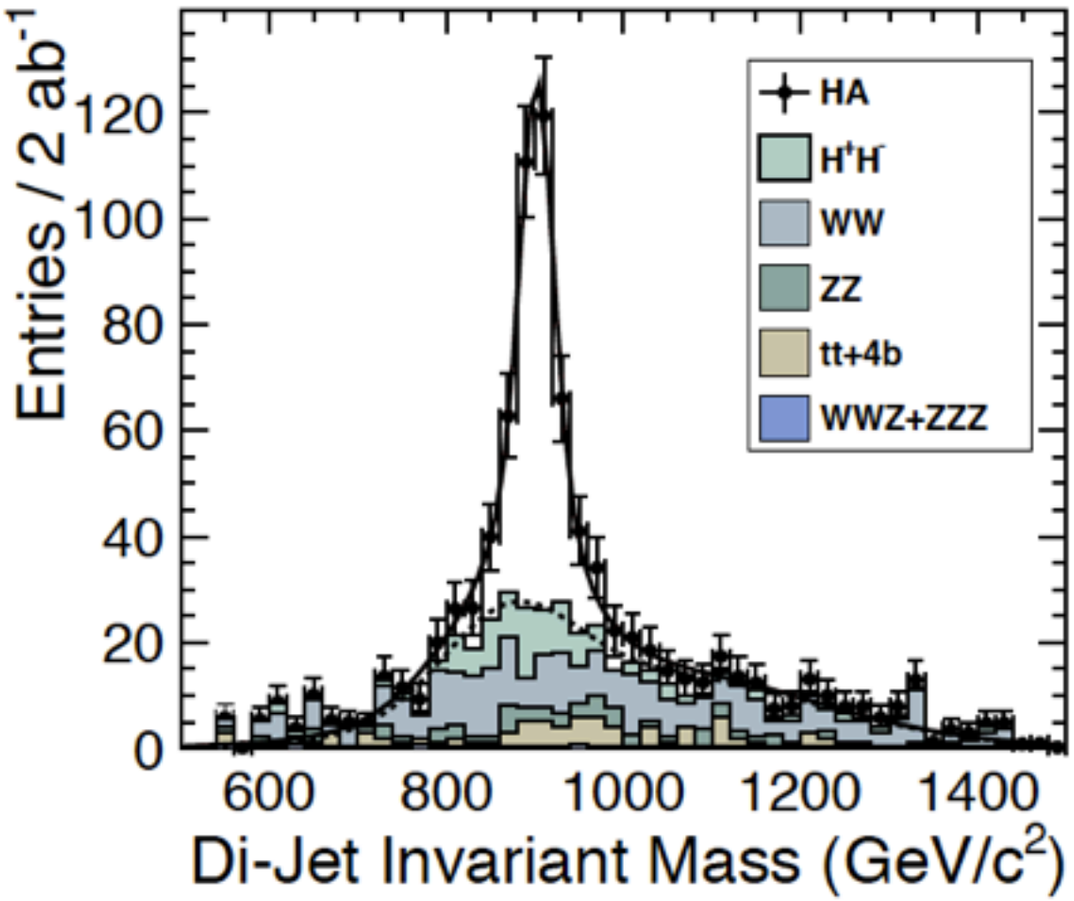

(a) $e^+e^- \to b\bar{b}b\bar{b}$

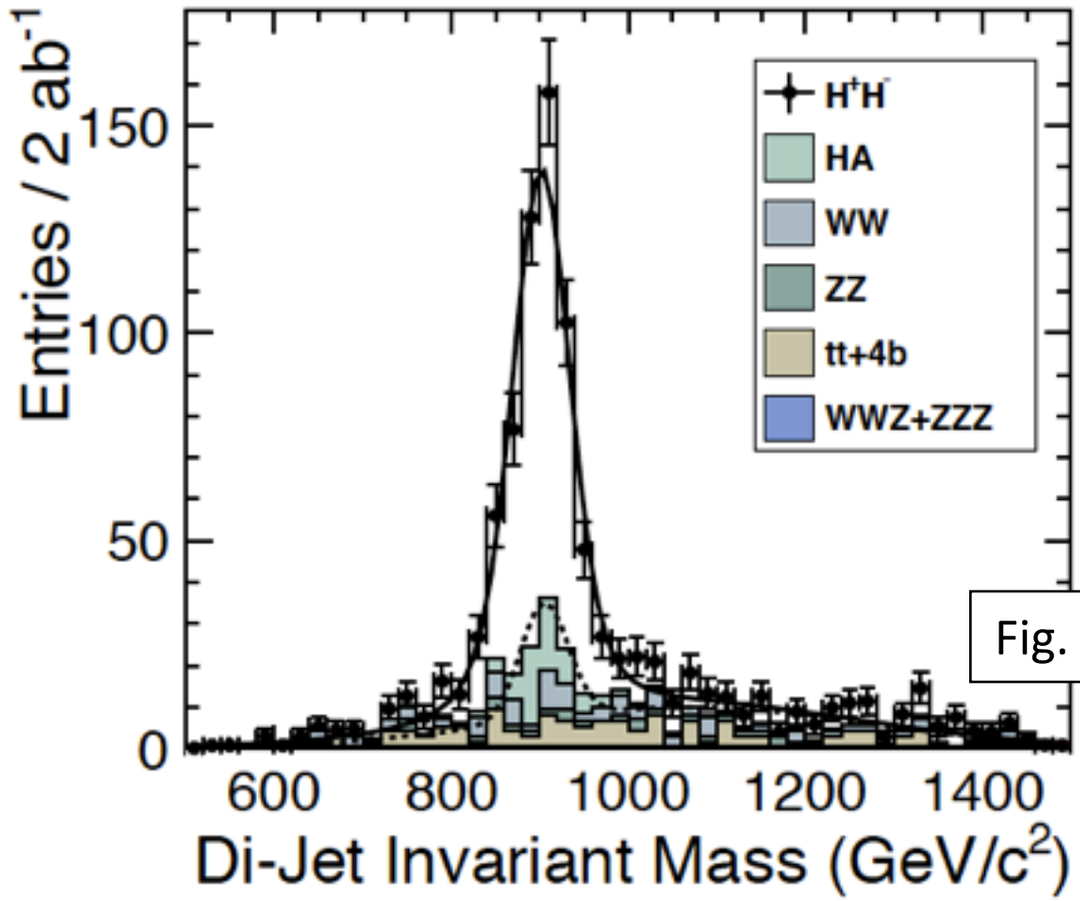

(b) $e^+e^- \to t\bar{b}b\bar{t}$

Fig. 12.20

	SUSY model I		*SUSY model II*	
State	Mass (GeV)	Width (GeV)	Mass (GeV)	Width GeV
A/H	904.5 ± 2.8	20.6 ± 6.3	743.7 ± 1.7	22.2 ± 3.8
$H^{\pm}$	902.6 ± 2.4	20.2 ± 5.4	746.9 ± 2.1	21.4 ± 4.9

- Masses and widths determined from fit with the sum of two BW, folded with Gaussian resolution function

Right-Squark Production

- Light-flavored squarks: typically among the heaviest SUSY particles - Jets + missing Energy as a generic new physics signature
  - Simple decay topology for right squarks:

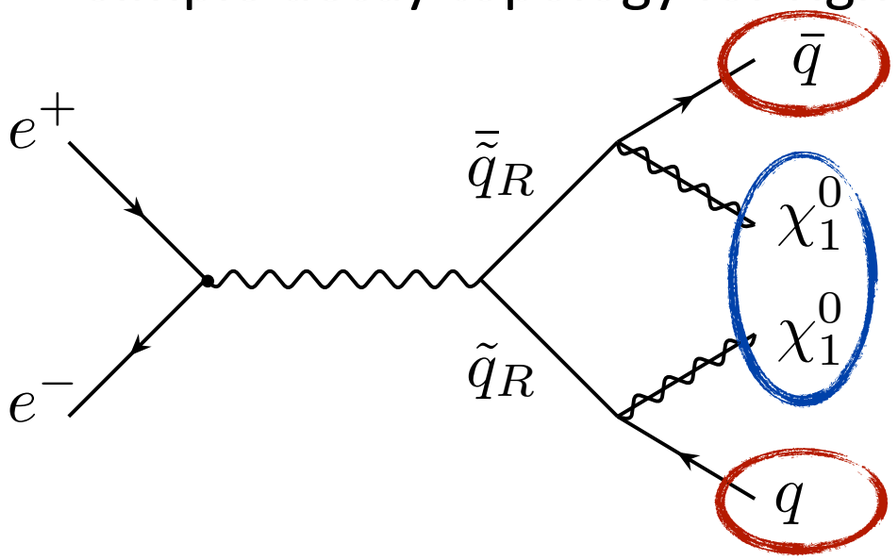

two highly energetic jets

missing energy

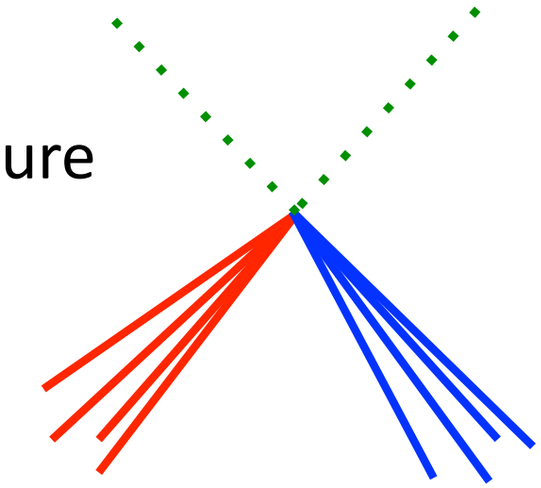

SUSY Model I: Right-Squark masses of 1.12 TeV (up & down -type nearly mass degenerate: 10 GeV mass splitting)

Cross section: 1.45 fb

Key detector performance aspects:

- Jet energy and missing energy reconstruction for high energy jets in a simple topology

CLIC_ILD

Right-Squarks - Analysis

- Main analysis challenges:
  - Suppression of SM background (4 orders of magnitude larger cross section than signal)
  - Jet finding in presence of background (see talk by M. Thomson)
- Strategy: Missing transverse momentum cut of 600 GeV, Boosted Decision Tree using jet and event shape information
- Mass measurement: $M_C = \sqrt{2(E_1 E_2 + \vec{p}_1 \cdot \vec{p}_2)}$ (independent of s)

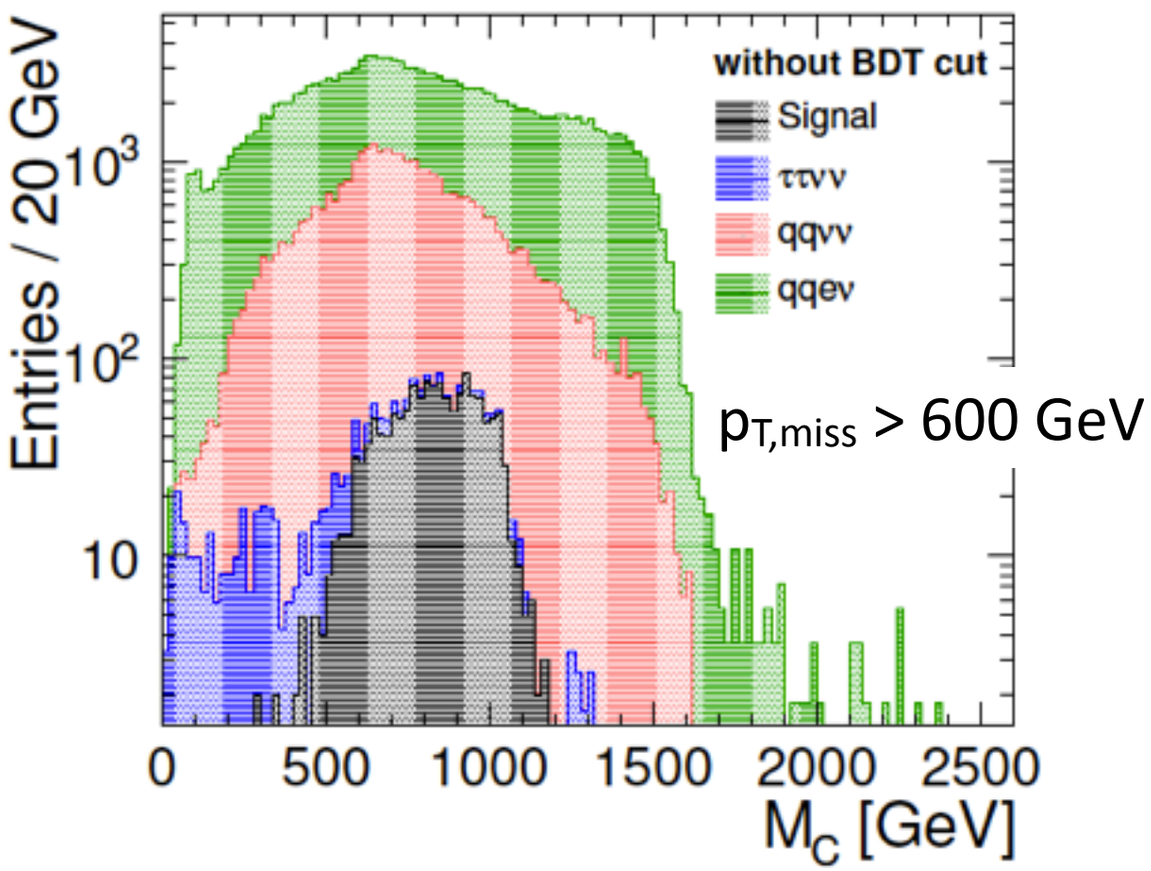

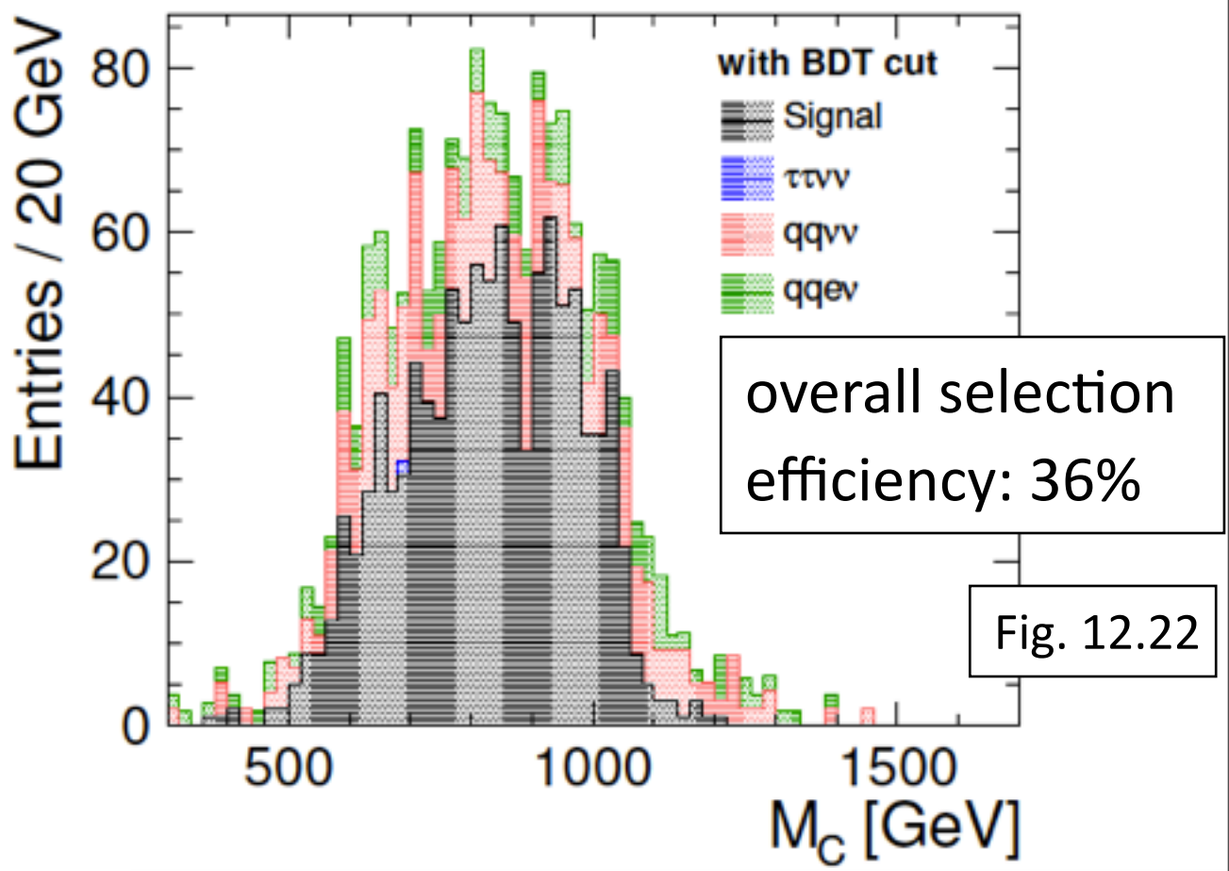

Fig. 12.22

Right Squarks - Results

- Mass determined with a template fit - Generator-level (including hadronization) simulations with various different squark masses, stat. errors from toy MC

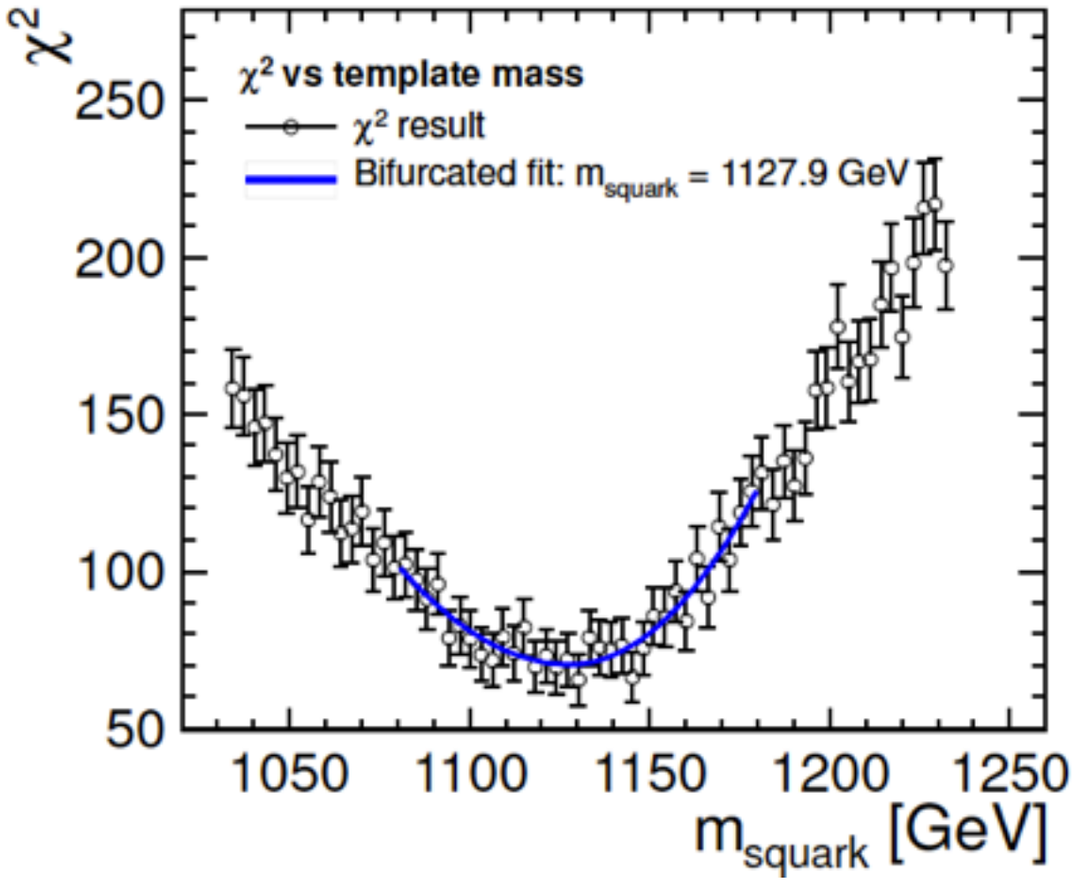

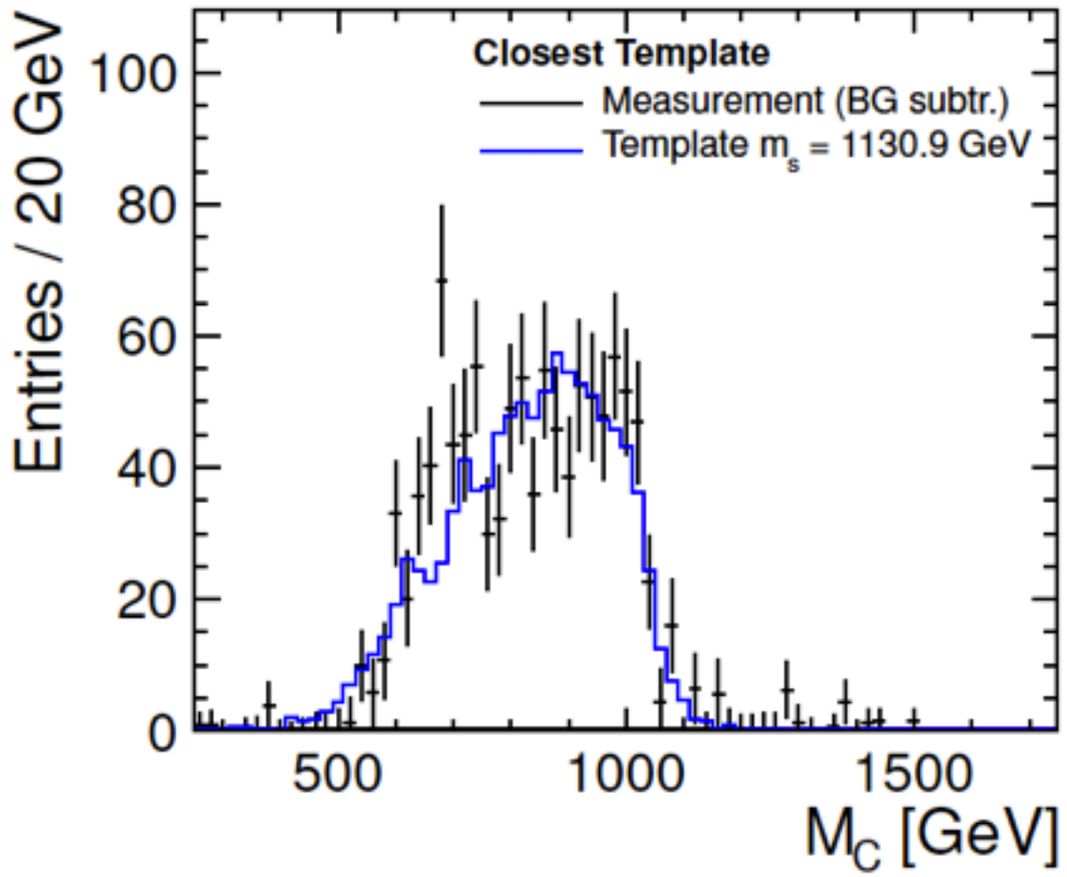

Fig. 12.23

Observable	Result	Generator value	
Averaged right-squark mass	1127.9 GeV ± 5.9 GeV	1123.7 GeV	0.52%
Combined cross section	1.51 fb ± 0.07 fb	1.47 fb	4.6 %

Slepton Production

- Sleptons - representative of generic NP signatures of leptons (+ jets) and missing energy
  - Decay topologies depending on process

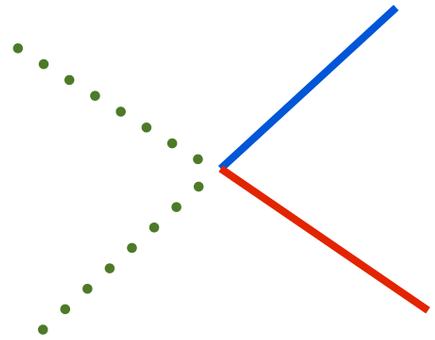

Process	σ (fb)	Decay Mode	$\sigma \times BR$ (fb)	$\sigma \times BR$ (ee4Q) (fb)
$e^+e^- \to \tilde{\mu}_R^+\tilde{\mu}_R^-$	0.72	$\mu^+\mu^-\tilde{\chi}_1^0\tilde{\chi}_1^0$	0.72	
$e^+e^- \to \tilde{e}_R^+\tilde{e}_R^-$	6.05	$e^+e^-\tilde{\chi}_1^0\tilde{\chi}_1^0$	6.05	
$e^+e^- \to \tilde{e}_L^+\tilde{e}_L^-$	3.07	$\tilde{\chi}_1^0\,\tilde{\chi}_1^0\,e^+e^-$ ($h/Z^0\,h/Z^0$)	0.25	0.16
$e^+e^- \to \tilde{\nu}_e\tilde{\nu}_e$	13.74	$\tilde{\chi}_1^0\,\tilde{\chi}_1^0 e^+e^-\,W^+W^-$	4.30	1.82

Key detector performance aspects:

- Reconstruction and identification of high energy leptons
- Energy resolution for high energy electrons and muons in two lepton and two lepton plus jets final states
- Boson mass resolution

SUSY model II:
slepton masses in the
1 TeV - 1.1 TeV range

CLIC_ILD

Slepton Production - Analysis

- Key analysis challenge: Rejection of SM background (3 to 4 orders of magnitude higher cross section than signal)

- Strategy:
  - Pre-selection cuts requiring high energy leptons inside detector acceptance with large di-lepton mass
  - Boosted Decision Tree using lepton energies, momenta, masses,acoplanarity

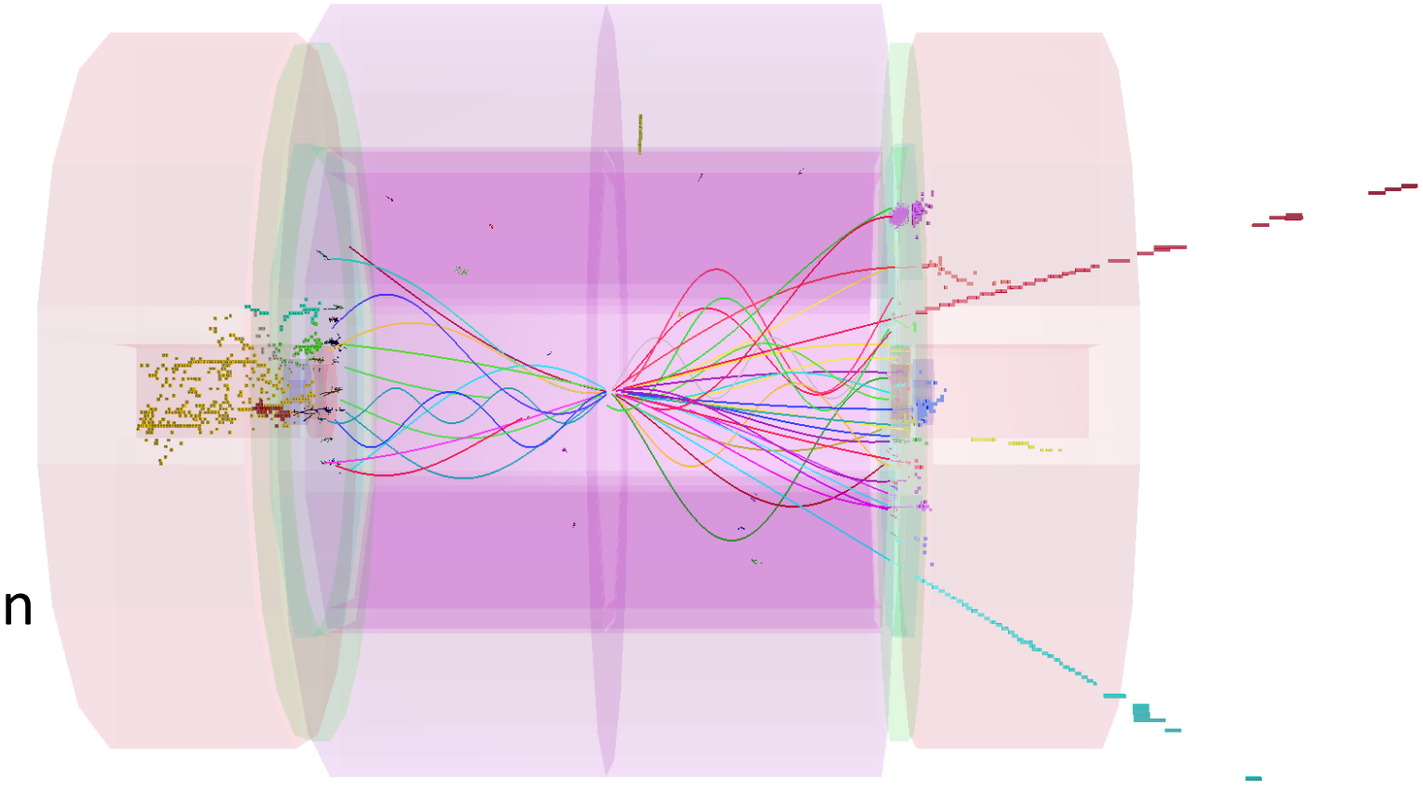

$$e^+e^- \to \tilde{\mu}_R^+\tilde{\mu}_R^- \to \mu^+\mu^-\tilde{\chi}_1^0\tilde{\chi}_1^0$$

Selection efficiencies of 97% for di-muon and 94% for di-electron final states

Slepton Production - Results

- Masses of sleptons and gauginos are extracted from kinematic edges
  - Fit using beam energy spectrum

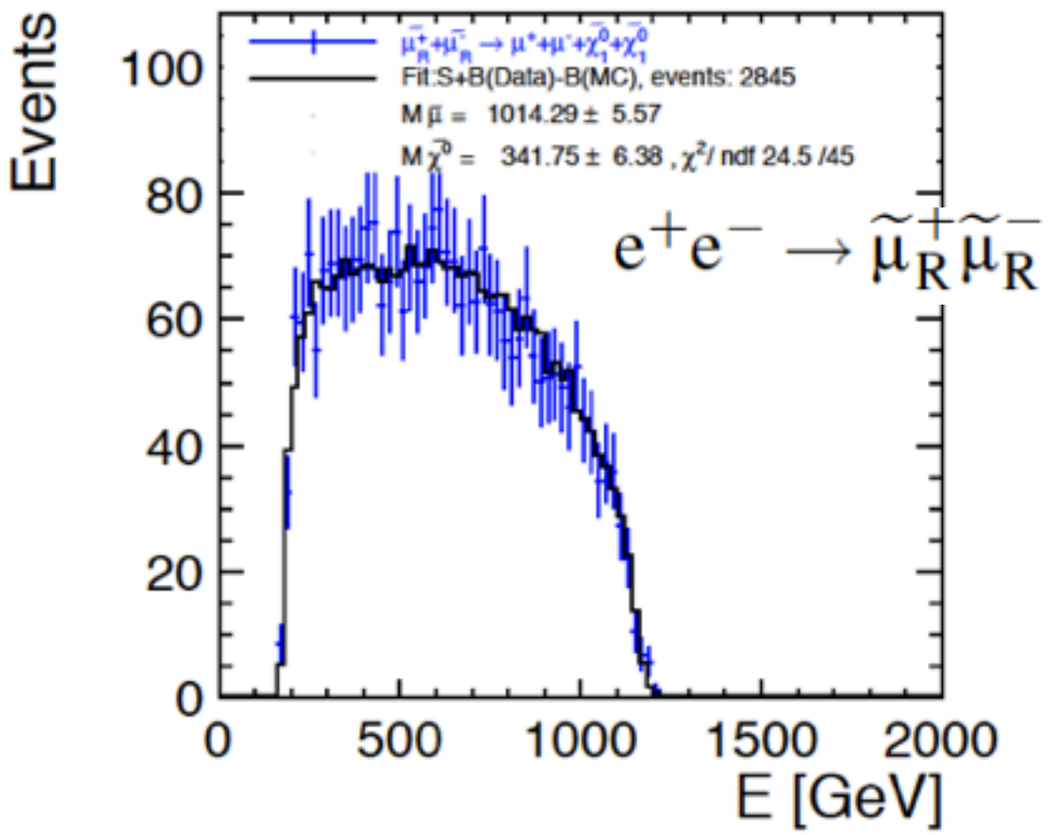

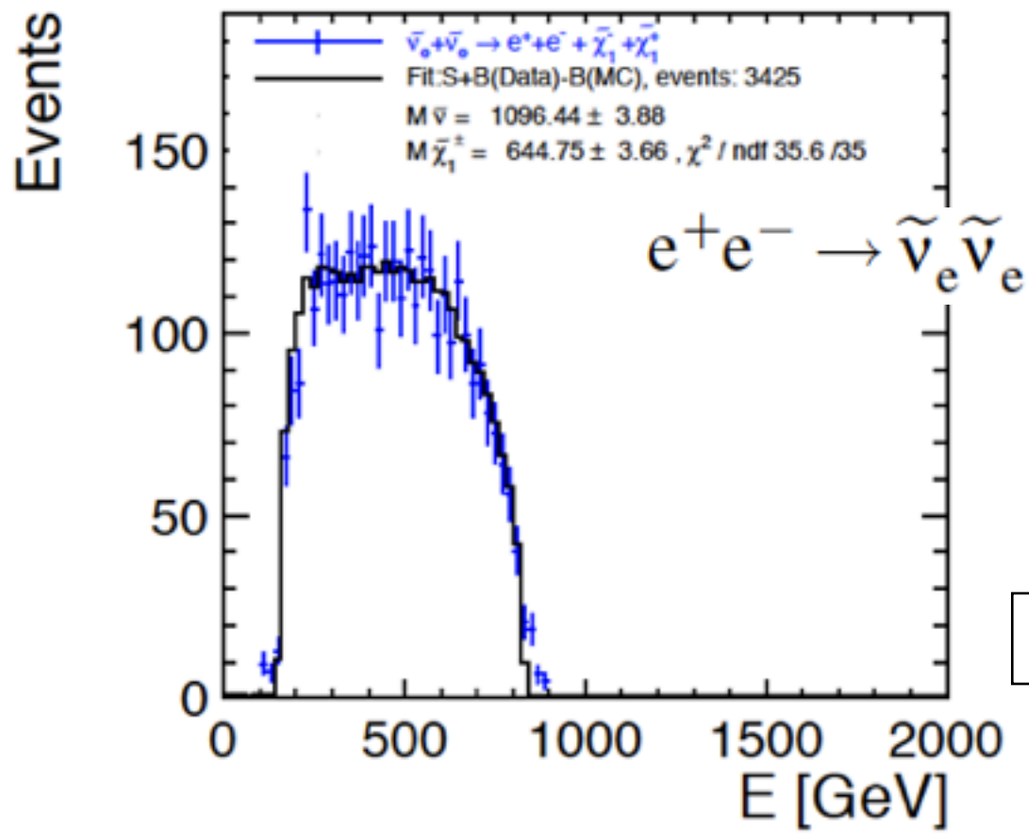

Fig. 12.24

Slepton Production - Results

- Masses of sleptons and gauginos are extracted from kinematic edges
  - Fit using beam energy spectrum

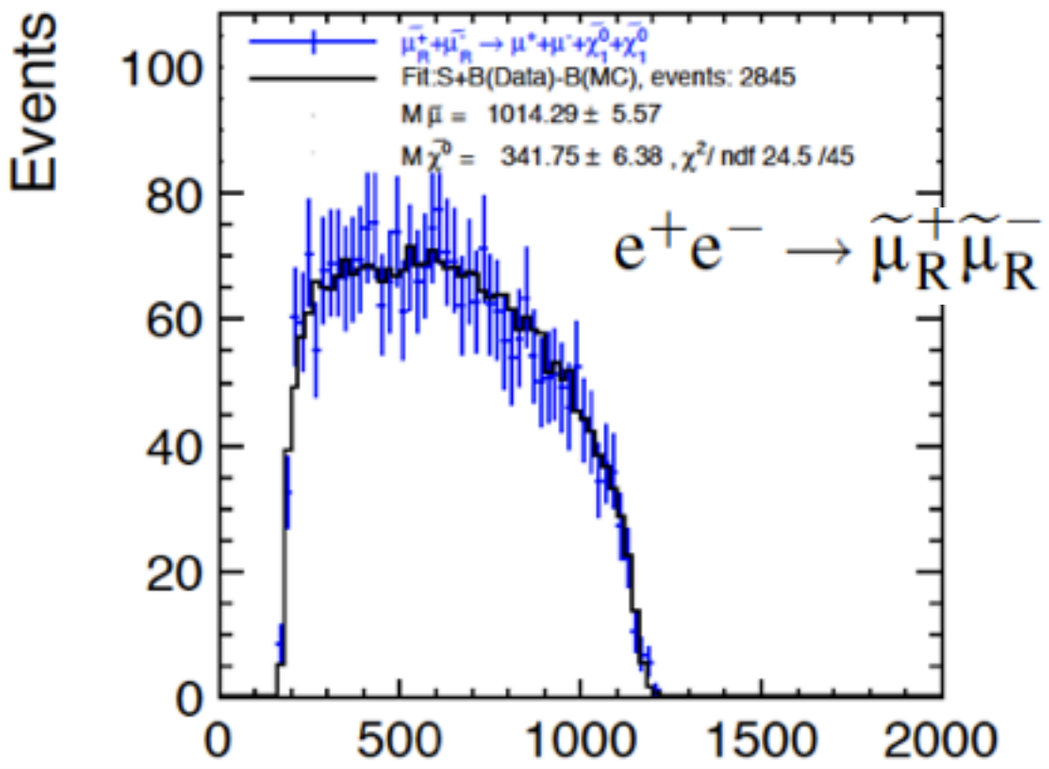

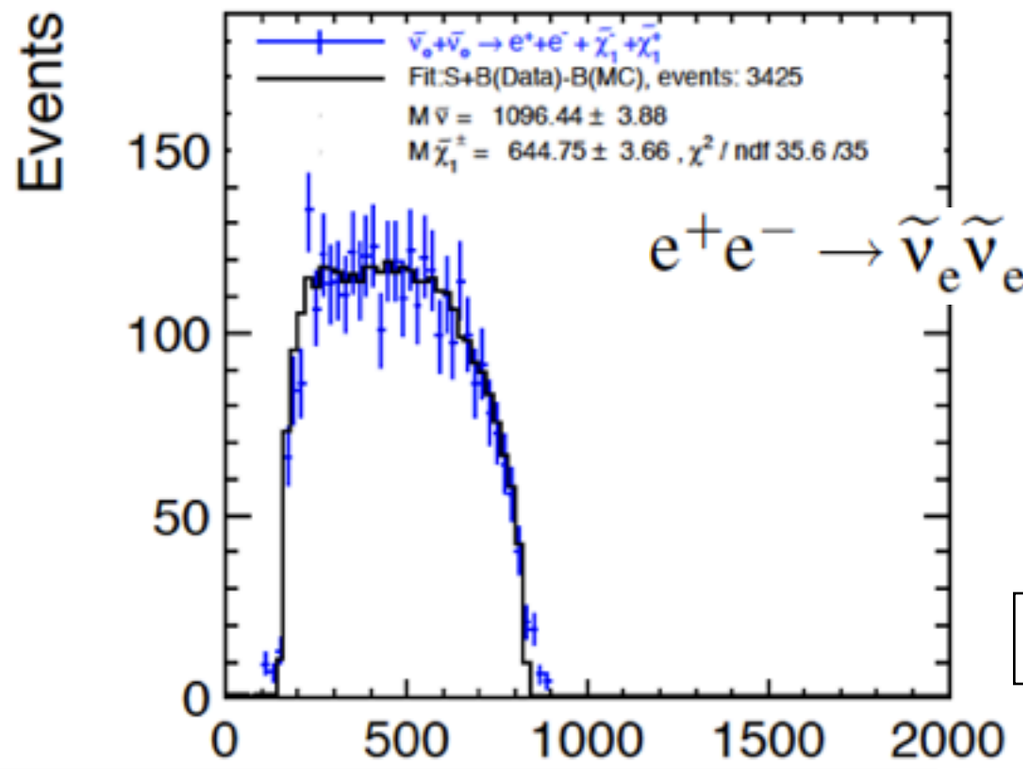

Fig. 12.24

Process	Decay Mode	σ (fb)	$m_{\tilde{\ell}}$ (GeV)	$m_{\tilde{\chi}_1^0}$ or $m_{\tilde{\chi}_1^\pm}$ (GeV)
$e^+e^- \to \tilde{\mu}_R^+\tilde{\mu}_R^-$	$\mu^+\mu^-\tilde{\chi}_1^0\tilde{\chi}_1^0$	0.71 ± 0.02	1014.3 ± 5.6	341.8 ± 6.4
$e^+e^- \to \tilde{e}_R^+\tilde{e}_R^-$	$e^+e^-\tilde{\chi}_1^0\tilde{\chi}_1^0$	6.20 ± 0.05	1001.6 ± 2.8	340.6 ± 3.4
$e^+e^- \to \tilde{e}_L^+\tilde{e}_L^-$	$\tilde{\chi}_1^0\,\tilde{\chi}_1^0\,e^+e^-$ ($h/Z^0\,h/Z^0$)	2.77 ± 0.20		
$e^+e^- \to \tilde{\nu}_e\tilde{\nu}_e$	$\tilde{\chi}_1^0\,\tilde{\chi}_1^0 e^+e^-\,W^+W^-$	13.24 ± 0.32	1096.4 ± 3.9	644.8 ± 3.7

Chargino & Neutralino Production

- Charginos & Neutralinos: Multi-jet final states with missing energy

$$e^+e^- \to \tilde{\chi}_1^+\tilde{\chi}_1^- \to W^+W^-\tilde{\chi}_1^0\tilde{\chi}_1^0$$
$$e^+e^- \to \tilde{\chi}_2^0\tilde{\chi}_2^0 \to h(Z)h(Z)\tilde{\chi}_1^0\tilde{\chi}_1^0$$

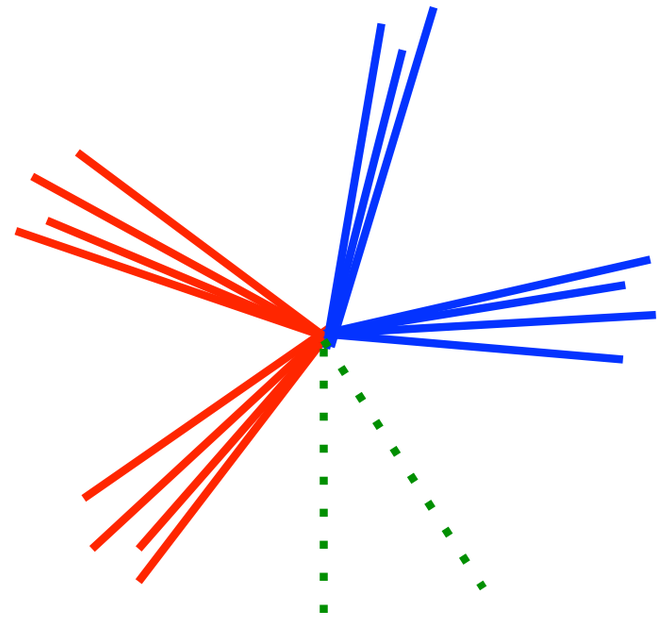

SUSY model II:
Chargino & Neutralino mass of 643 GeV

Key detector performance aspects:
- Jet energy and missing energy reconstruction in high energy decays
- Di-Jet mass reconstruction and separation of hadronic Z, W and h decays

CLIC_SiD

Chargino & Neutralino - Analysis

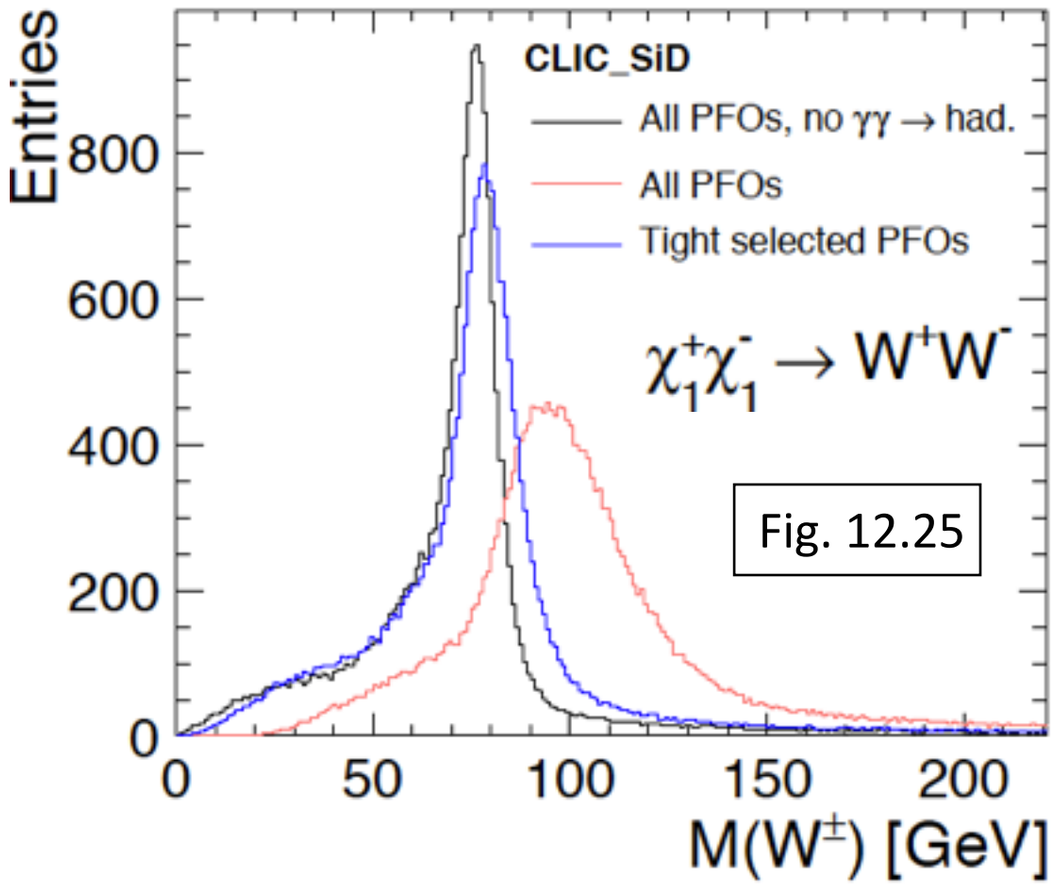

Fig. 12.25

- Background rejection using a Boosted Decision Tree
  - Efficiency for Charginos 33%, for Neutralinos 25%; Purity approximately 56%

- Key challenge: Separation of heavy bosons in hadronic final states in the presence of background

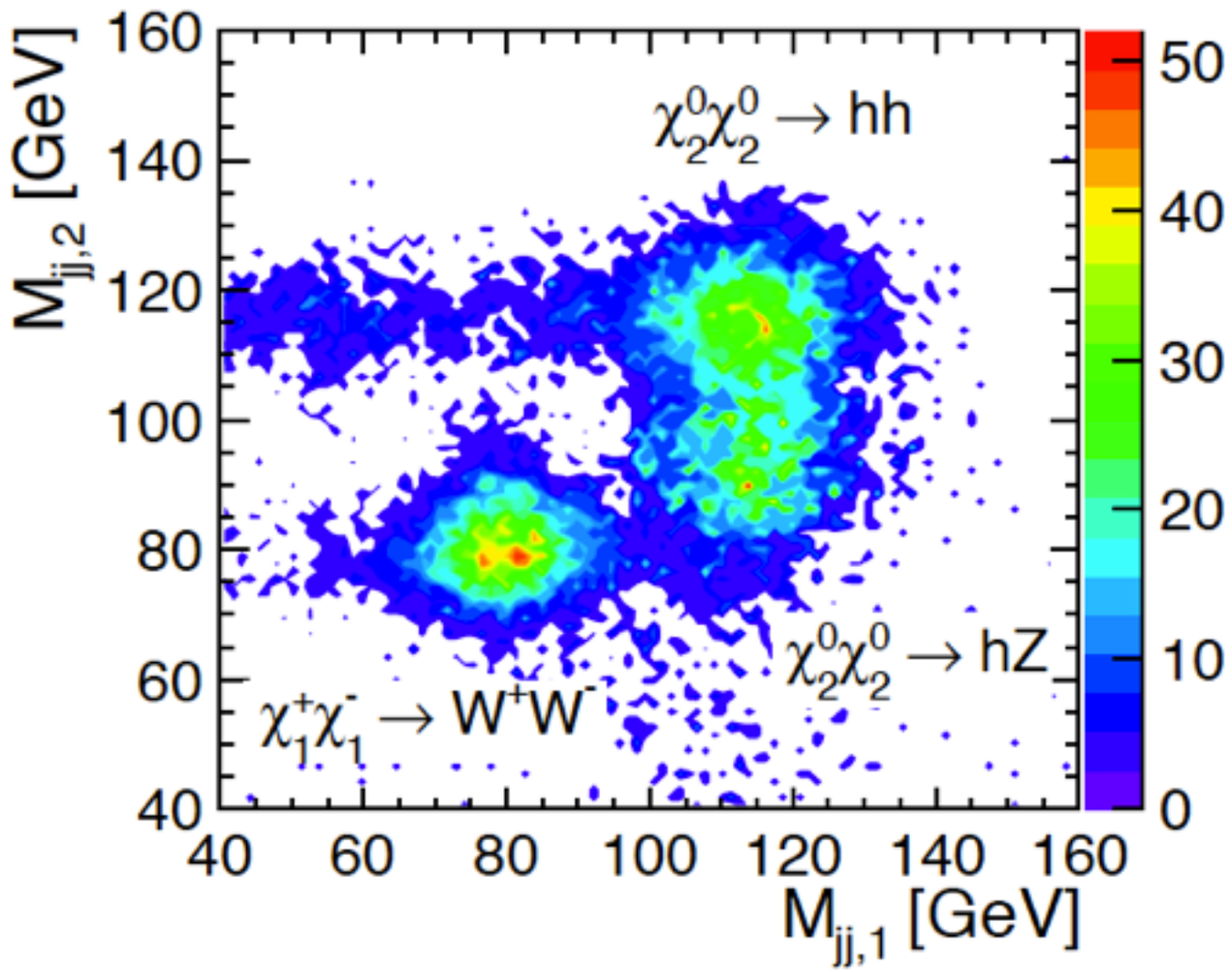

Fig. 12.9

Chargino & Neutralino - Analysis

- Mass and cross section from template (fully simulated) and least squares fits to boson energy distribution - provides also sensitivity to LSP mass

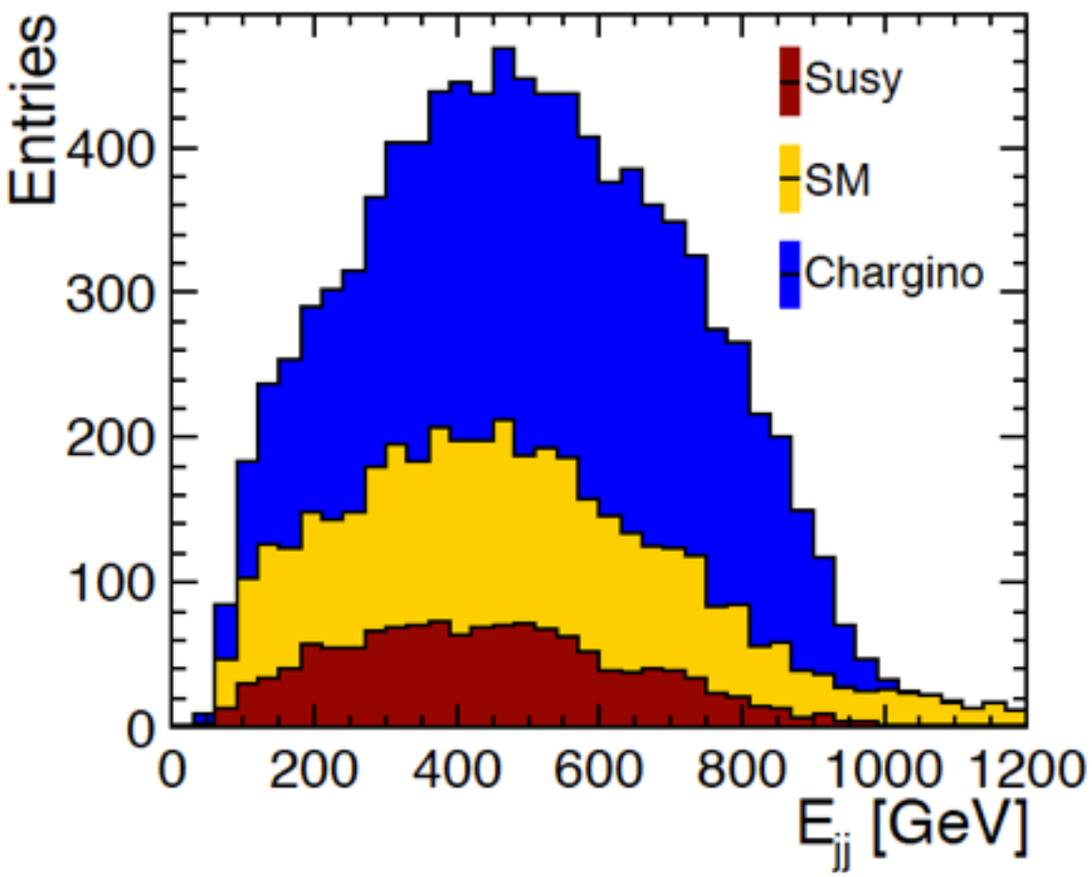

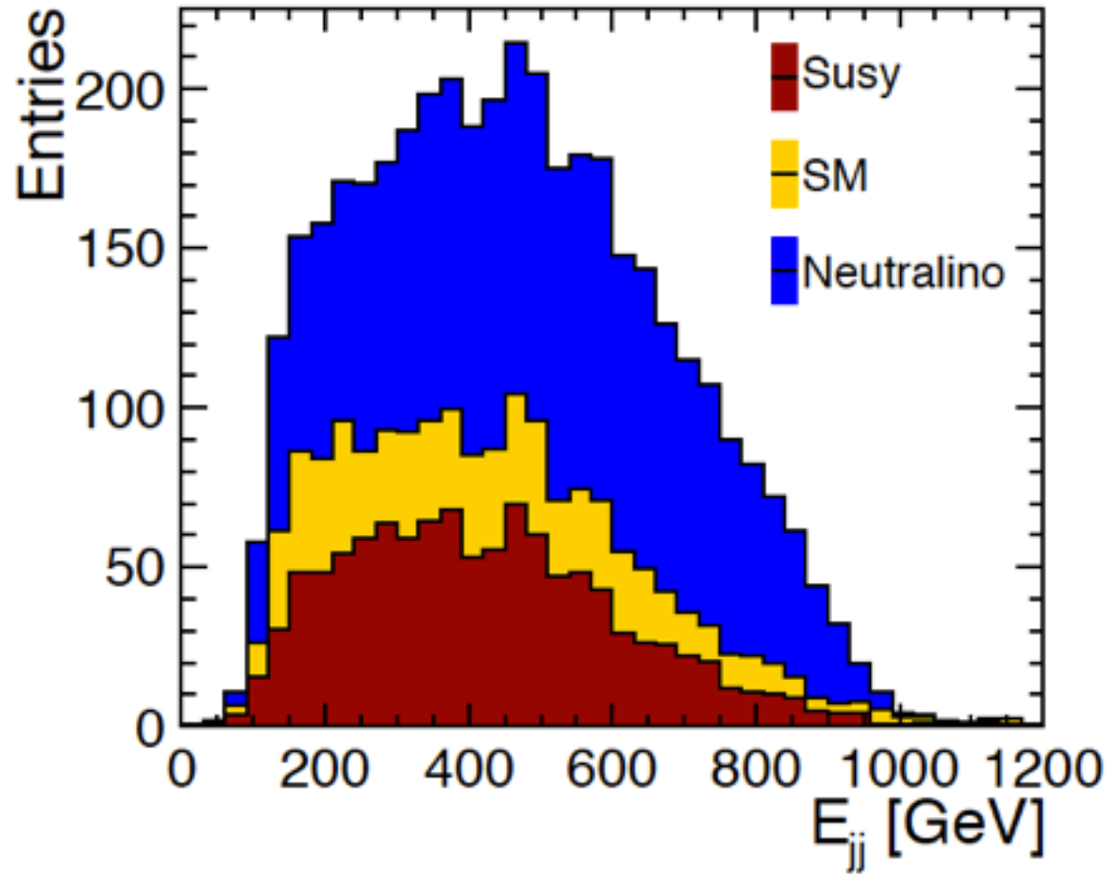

Parameter 1	Uncertainty	Parameter 2	Uncertainty
$M(\tilde{\chi}_1^{\pm})$	6.3 GeV	$\sigma(\tilde{\chi}_1^+\tilde{\chi}_1^-)$	2.2%
$M(\tilde{\chi}_1^0)$	3.0 GeV	$\sigma(\tilde{\chi}_1^+\tilde{\chi}_1^-)$	1.8%
$M(\tilde{\chi}_2^0)$	7.3 GeV	$\sigma(\tilde{\chi}_2^0\tilde{\chi}_2^0)$	2.9%

Fig. 12.26, 27

consistent results with least squares fit

500 GeV Benchmark

- Assumed integrated luminosity of 100 fb^{-1}
- Full detector simulations with a modified detector model

Detector Modifications at 500 GeV

- The background conditions at 500 GeV are substantially less severe than at 3 TeV

- Lower rate of incoherent pairs (8×10^4/BX vs 3×10^5/BX): Allows a reduction of the beam pipe radius at the IP, and a smaller radius of the vertex detector (25 mm vs 31 mm): Improved flavor tagging for lower jet energies

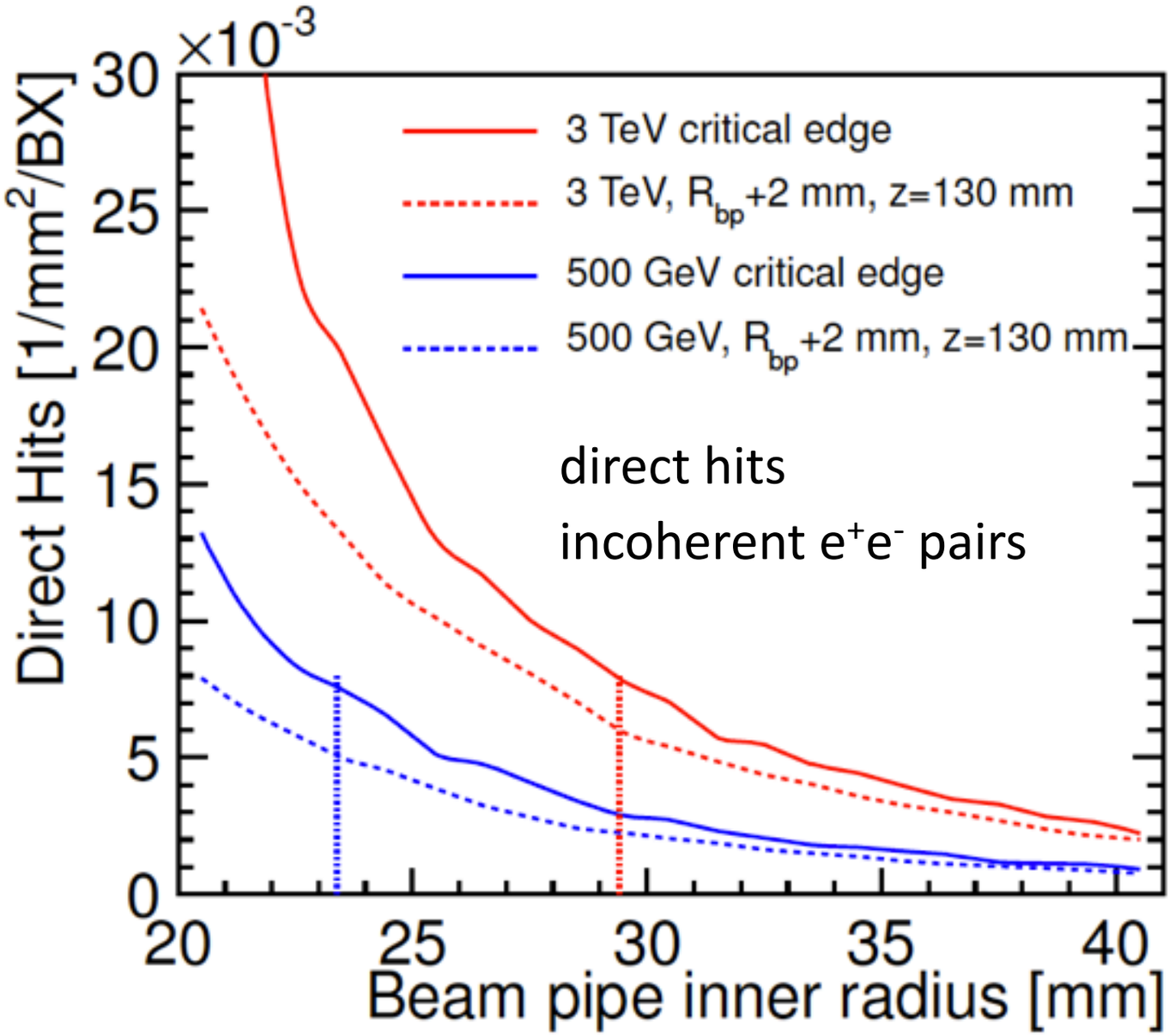

LCD-Note-2011-021

Detector Modifications at 500 GeV

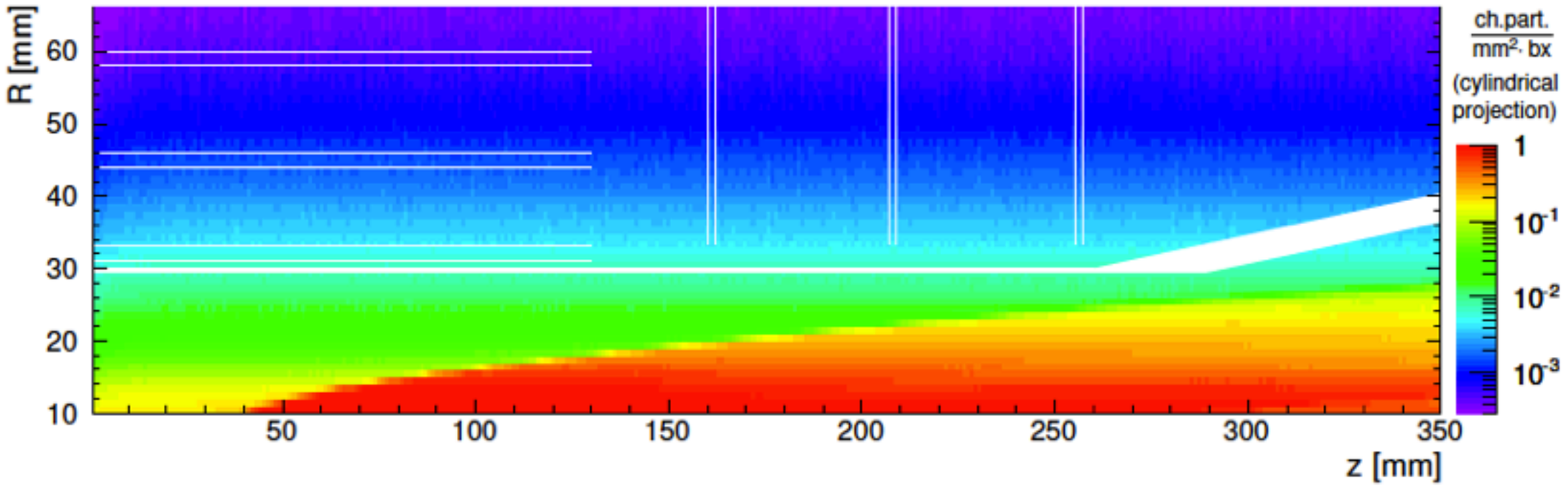

(a) $\sqrt{s} = 3$ TeV

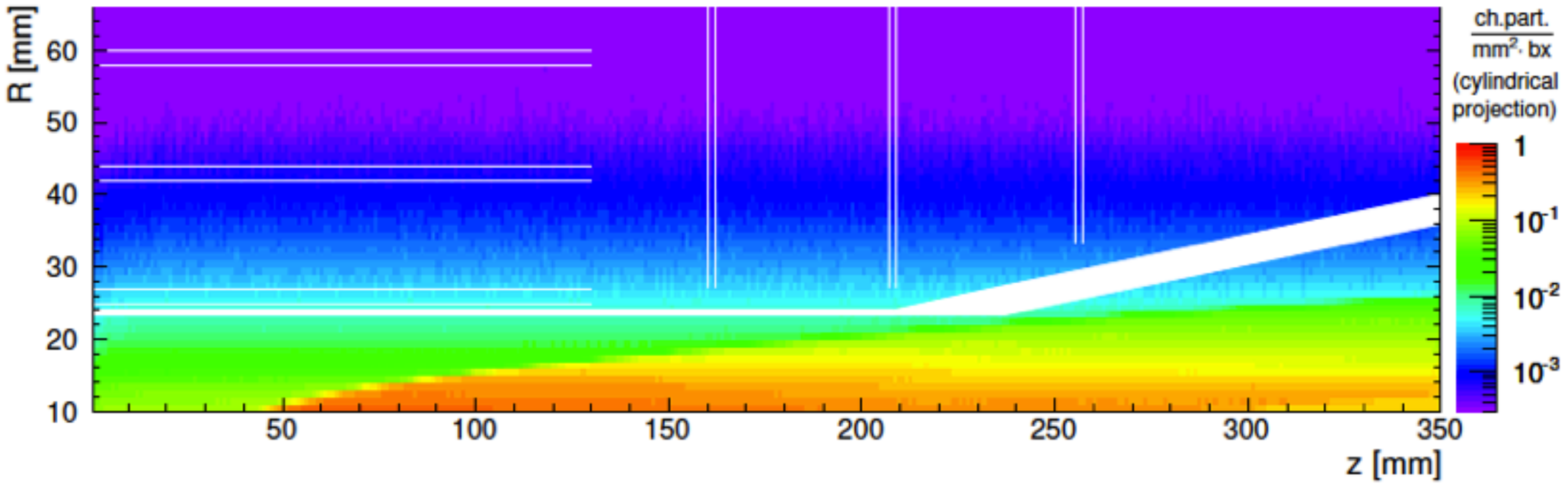

(b) $\sqrt{s} = 500$ GeV

LCD-Note-2011-021

- Incoherent pairs in the vertex region: 500 GeV vs 3 TeV

Event Reconstruction at 500 GeV

- The background conditions at 500 GeV are substantially less severe than at 3 TeV
  - Most important for physics analysis:
    - Lower rate of hadronic background: 0.19/BX vs 3.2/BX

      Relaxed timing and momentum cuts: Important to recover energy resolution for lower energy jets
    - Smaller beam energy spread: 61% of total L in top 1%

      Allows kinematic fitting assuming energy conservation for processes with invisible particles in the final state

Event Reconstruction at 500 GeV

500 GeV - Default cuts

Region	p_t *range*	Time cut
Photons		
central ($\cos\theta \leq 0.975$)	$1.0\ \text{GeV} \leq p_t < 2.0\ \text{GeV}$ $0\ \text{GeV} \leq p_t < 1.0\ \text{GeV}$	$t < 5.0$ nsec $t < 2.5$ nsec
forward ($\cos\theta > 0.975$)	$0.75\ \text{GeV} \leq p_t < 4.0\ \text{GeV}$ $0\ \text{GeV} \leq p_t < 0.75\ \text{GeV}$	$t < 2.0$ nsec $t < 1.0$ nsec
Neutral hadrons		
central ($\cos\theta \leq 0.975$)	$1.0\ \text{GeV} \leq p_t < 2.0\ \text{GeV}$ $0\ \text{GeV} \leq p_t < 1.0\ \text{GeV}$	$t < 5.0$ nsec $t < 2.5$ nsec
forward ($\cos\theta > 0.975$)	$2.0\ \text{GeV} \leq p_t < 4.0\ \text{GeV}$ $0\ \text{GeV} \leq p_t < 2.0\ \text{GeV}$	$t < 2.0$ nsec $t < 1.0$ nsec
Charged PFOs		
all	$1.0\ \text{GeV} \leq p_t < 4.0\ \text{GeV}$ $0\ \text{GeV} \leq p_t < 1.0\ \text{GeV}$	$t < 10.0$ nsec $t < 3.0$ nsec

3 TeV - Default

extends to higher p_t
2.0 ns & 1.0 ns

same

extends to higher p_t
2.5 ns & 1.5 ns

extends to higher p_t
same time cuts

3.0 ns & 1.5 ns

LCD-Note-2011-026

Event Reconstruction at 500 GeV

- Influence of timing cuts and background:
  - top pair events (all decay modes)

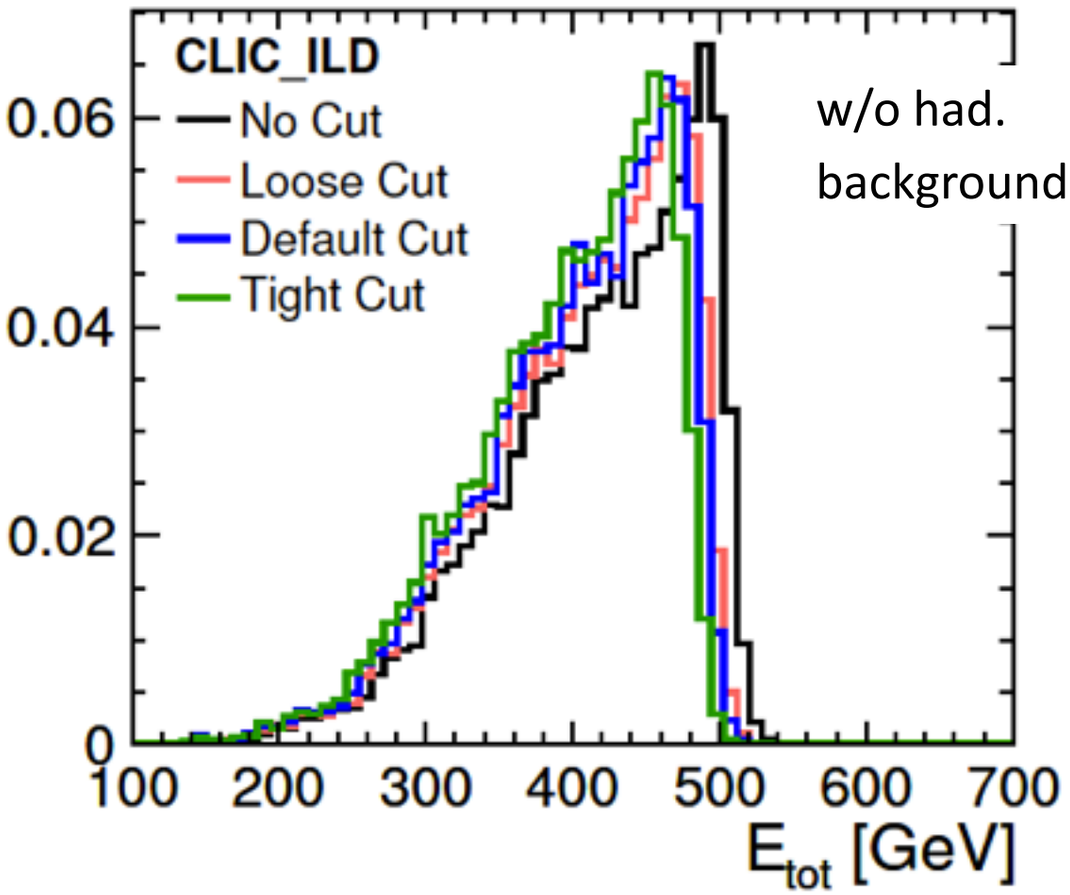

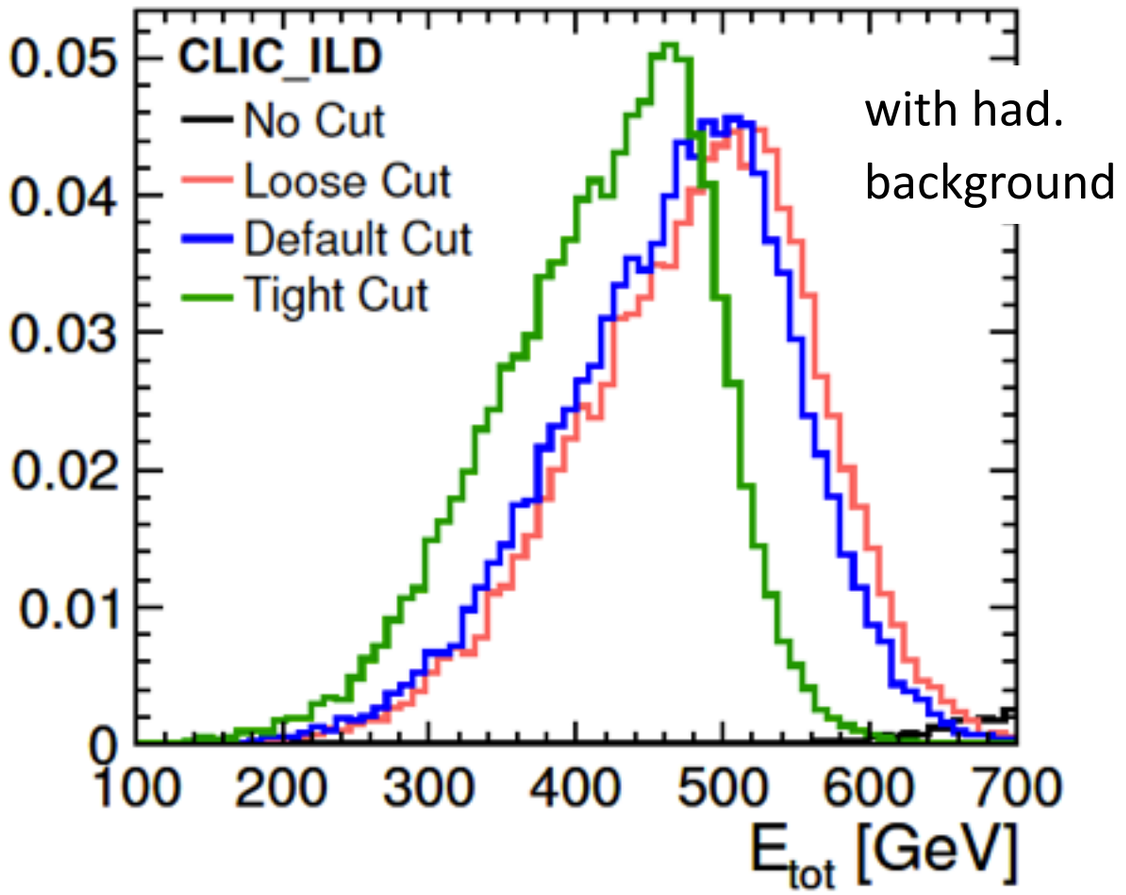

LCD-Note-2011-026

Top Pair Production at 500 GeV

- Top mass and width - a classic Standard Model measurement at Linear Colliders
  - Multi-jet final state at ILC energies

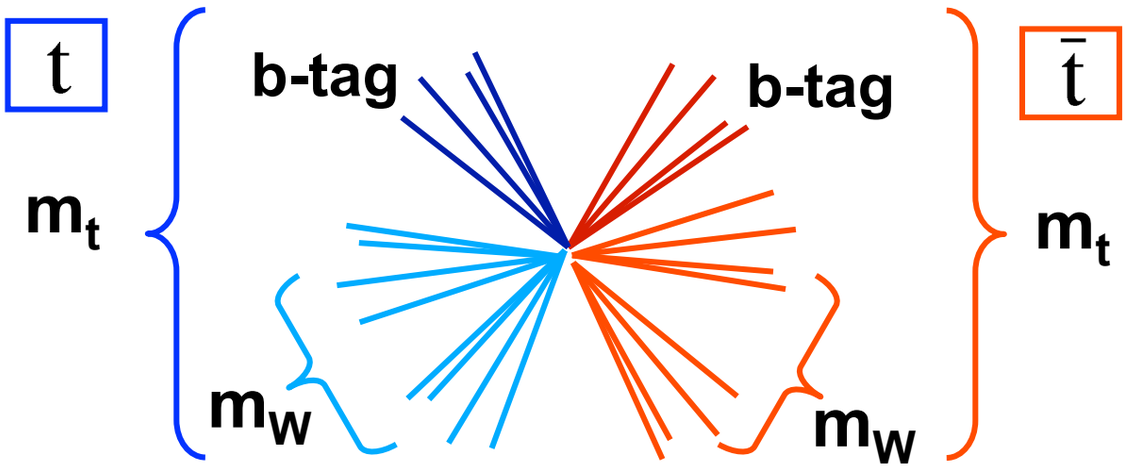

Key detector performance aspects:

- Mass reconstruction in a multi-jet final state for low energy jets
- Flavor tagging

In addition: Evaluation of the impact of CLIC beam conditions at 500 GeV compared to those of the ILC

CLIC_ILD

Top Pairs - Analysis

- Analysis focus: Precise determination of the top mass
- Strategy:
  - Selection of fully hadronic and semi-leptonic top pair candidates, jet finding with fixed number of jets
  - Flavor tagging to identify b-quarks
  - Kinematic fit using energy and momentum constraints to improve mass resolution and to find correct assignment of b quarks and W bosons into top candidates
- Backgrounds:
  - Di- and tri-boson production, quark pair production
  - Effectively rejected by kinematic fit, further reduced with a likelihood technique

Top Pairs - Results

- Unbinned maximum likelihood fit of mass distributions

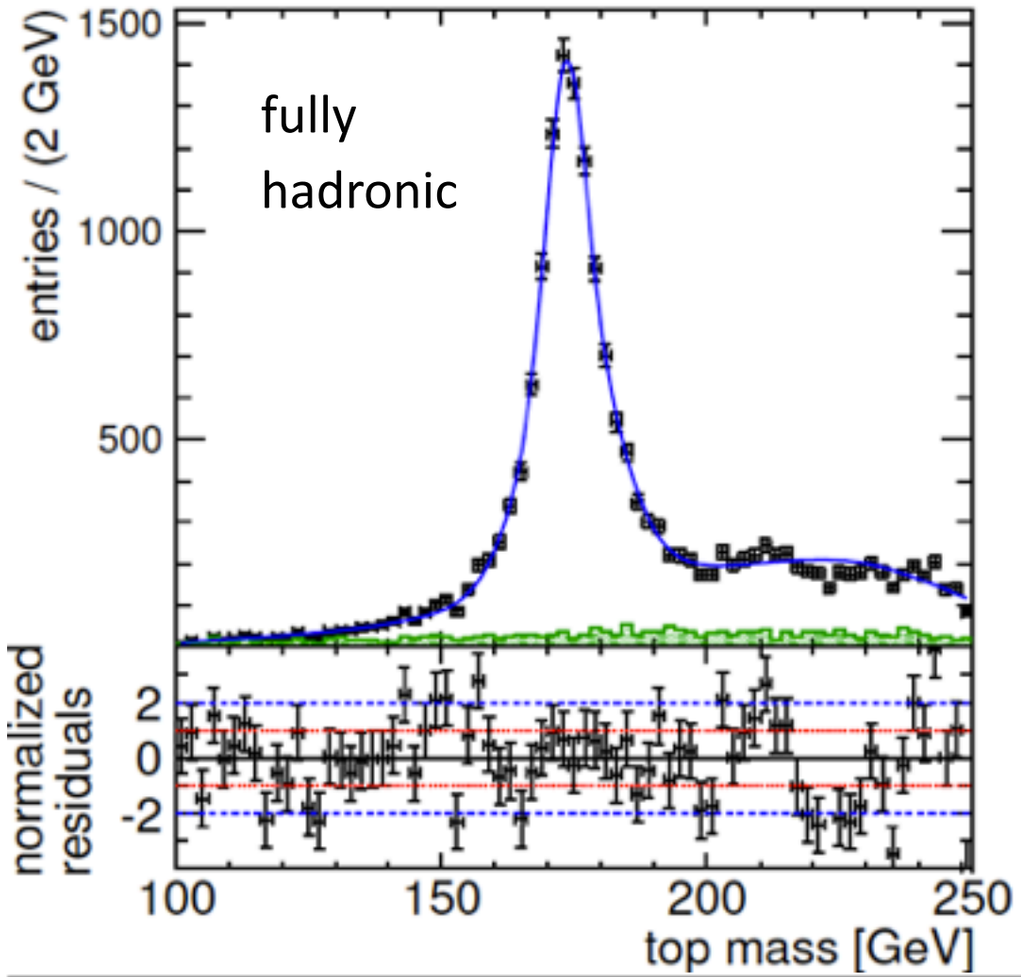

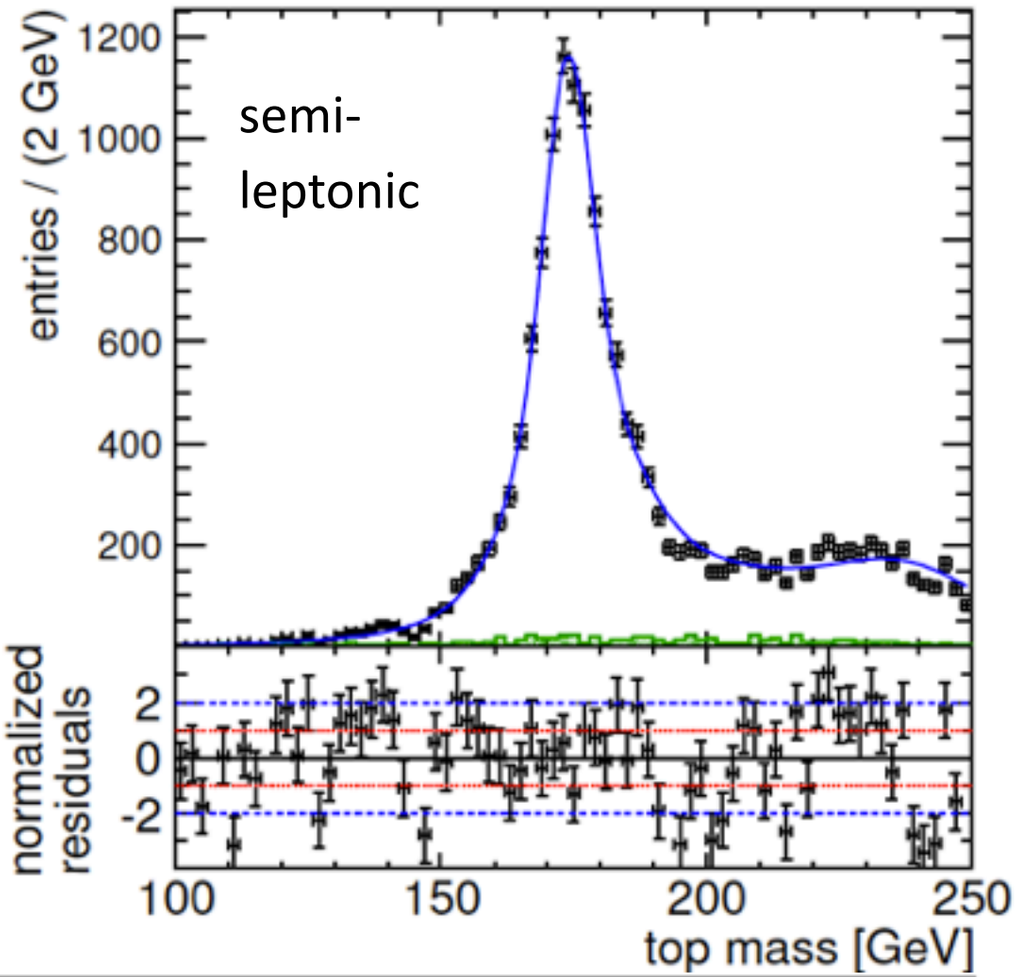

Top decay	Top mass (GeV)	Top width (GeV)	Generator value	
			Mass (GeV)	Width (GeV)
Fully-hadronic	174.08 ± 0.08	1.42 ± 0.22	174	1.37
Semi-leptonic	174.30 ± 0.09	1.45 ± 0.26		

Comparable to ILD LOI mass resolution (0.11 GeV in all-hadronic final state)

Summary

- Physics benchmark studies have shown:
  - Precision studies of high-mass states and complicated final states are possible at CLIC
  - At 500 GeV, similar mass measurement precision for high-multiplicity final states can be reached as with ILC

- Additional topics for study:

  Systematic uncertainties - All present studies show statistical errors only

Results Summary

$\sqrt{s}$ (TeV)	Process	Decay mode	SUSY model	Observable	Unit	Generator value	Stat. uncertainty
3.0	Light Higgs production	$h \to b\bar{b}$ $h \to c\bar{c}$ $h \to \mu^+\mu^-$		σ $\times$ Branching ratio	fb	285 13 0.12	0.22% 3.2% 23%
3.0	Heavy Higgs production	$HA \to b\bar{b}b\bar{b}$	I	Mass Width	GeV GeV	902.4	0.3% 31%
			II	Mass Width	GeV GeV	742.0	0.2% 17%
		$H^+H^- \to t\bar{b}b\bar{t}$	I	Mass Width	GeV GeV	906.3	0.3% 27%
			II	Mass Width	GeV GeV	747.6	0.3% 23%
3.0	Production of right-handed squarks	$\tilde{q}_R\tilde{q}_R \to q\bar{q}\tilde{\chi}_1^0\tilde{\chi}_1^0$	I	Mass σ	GeV fb	1123.7 1.47	0.52% 4.6%

Results Summary

$\sqrt{s}$ (TeV)	Process	Decay mode	SUSY model	Observable	Unit	Generator value	Stat. uncertainty
3.0	Sleptons production	$\tilde{\mu}_R^+\tilde{\mu}_R^- \to \mu^+\mu^-\tilde{\chi}_1^0\tilde{\chi}_1^0$	II	σ	fb	0.72	2.8%
				$\tilde{\ell}$ mass	GeV	1010.8	0.6%
				$\tilde{\chi}_1^0$ mass	GeV	340.3	1.9%
		$\tilde{e}_R^+\tilde{e}_R^- \to e^+e^-\tilde{\chi}_1^0\tilde{\chi}_1^0$		σ	fb	6.05	0.8%
				$\tilde{\ell}$ mass	GeV	1010.8	0.3%
				$\tilde{\chi}_1^0$ mass	GeV	340.3	1.0%
		$\tilde{e}_L^+\tilde{e}_L^- \to \tilde{\chi}_1^0\tilde{\chi}_1^0 e^+e^- hh$ $\tilde{e}_L^+\tilde{e}_L^- \to \tilde{\chi}_1^0\tilde{\chi}_1^0 e^+e^- Z^0Z^0$		σ	fb	3.07	7.2%
		$\tilde{\nu}_e\tilde{\nu}_e \to \tilde{\chi}_1^0\tilde{\chi}_1^0 e^+e^- W^+W^-$		σ	fb	13.74	2.4%
				$\tilde{\ell}$ mass	GeV	1097.2	0.4%
				$\tilde{\chi}_1^\pm$ mass	GeV	643.2	0.6%
3.0	Chargino and neutralino production	$\tilde{\chi}_1^+\tilde{\chi}_1^- \to \tilde{\chi}_1^0\tilde{\chi}_1^0 W^+W^-$	II	$\tilde{\chi}_1^\pm$ mass	GeV	643.2	1.1%
				σ	fb	10.6	2.4%
		$\tilde{\chi}_2^0\tilde{\chi}_2^0 \to h^0/Z^0h^0/Z^0\tilde{\chi}_1^0\tilde{\chi}_1^0$		$\tilde{\chi}_2^0$ mass	GeV	643.1	1.5%
				σ	fb	3.3	3.2%
0.5	$t\bar{t}$ production	$t\bar{t} \to (q\bar{q}b)\,(q\bar{q}b)$		Mass	GeV	174	0.046%
				Width	GeV	1.37	16%
		$t\bar{t} \to (q\bar{q}b)\,(\ell\nu b)$, $\ell = e, \mu$		Mass	GeV	174	0.052%
				Width	GeV	1.37	18%

Backup

3 TeV PFO Cuts

3 TeV Default Cuts

Region	p_T range	time cut
	Photons	
central	$0.75\ \text{GeV} \leq p_T < 4.0\ \text{GeV}$	$t < 2.0$ ns
$\cos\theta \leq 0.975$	$0\ \text{GeV} \leq p_T < 0.75\ \text{GeV}$	$t < 1.0$ ns
forward	$0.75\ \text{GeV} \leq p_T < 4.0\ \text{GeV}$	$t < 2.0$ ns
$\cos\theta > 0.975$	$0\ \text{GeV} \leq p_T < 0.75\ \text{GeV}$	$t < 1.0$ ns
	neutral hadrons	
central	$0.75\ \text{GeV} \leq p_T < 8.0\ \text{GeV}$	$t < 2.5$ ns
$\cos\theta \leq 0.975$	$0\ \text{GeV} \leq p_T < 0.75\ \text{GeV}$	$t < 1.5$ ns
forward	$0.75\ \text{GeV} \leq p_T < 8.0\ \text{GeV}$	$t < 2.0$ ns
$\cos\theta > 0.975$	$0\ \text{GeV} \leq p_T < 0.75\ \text{GeV}$	$t < 1.0$ ns
	charged particles	
all	$0.75\ \text{GeV} \leq p_T < 4.0\ \text{GeV}$	$t < 3.0$ ns
	$0\ \text{GeV} \leq p_T < 0.75\ \text{GeV}$	$t < 1.5$ ns